9th World Congress of Biomechanics
2022 Taipei
Taipei International Convention Center

Modelling the apparent viscoelastic behaviour of passive muscle tissue under confined compression using a poroelastic framework

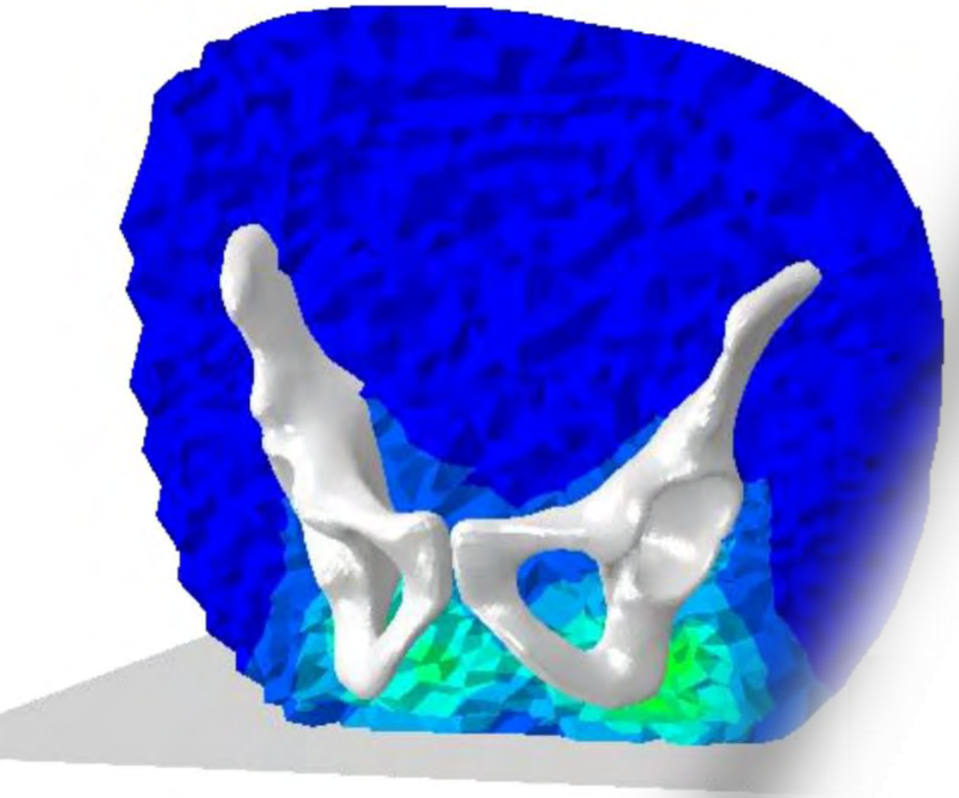

[Macron et al., 2018]

Thomas Lavigne, Giuseppe Sciumè,
Sébastien Laporte, Hélène Pillet,
Stéphane Urcun , Benjamin Wheatley, Pierre-Yves Rohan

| SB 2021– Ocotber 2021

Corresponding author: thomas.lavigne@ext.uni.lu

Context

Pressure ulcers:
- Localized injury
- Long terme and/or excessive loading [Bouten et al., 2003]

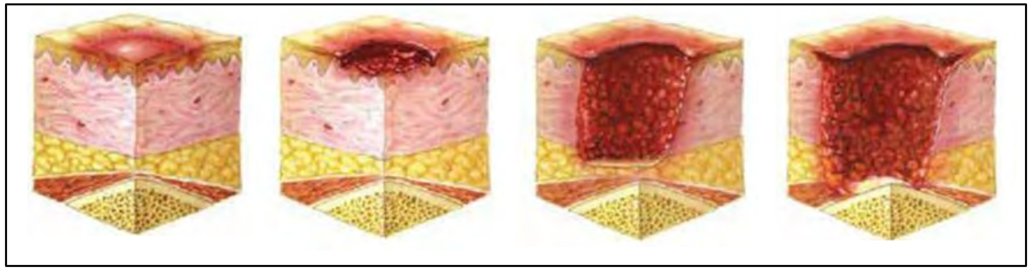

Stages 1 to 4 of pressure ulcers
[winncareacademy.com]

Context

Pressure ulcers:
- Localized injury
- Long terme and/or excessive loading [Bouten et al., 2003]

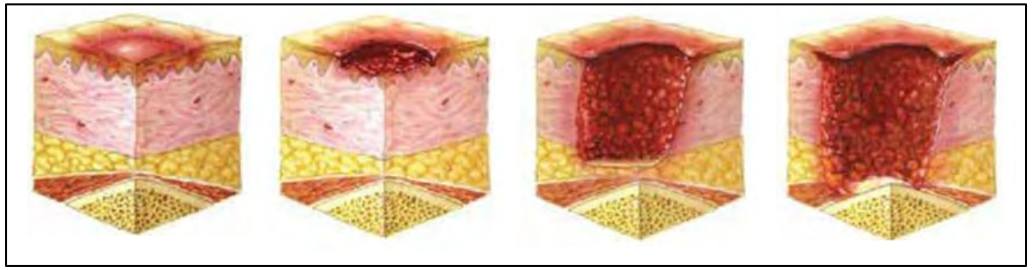

Stages 1 to 4 of pressure ulcers
[winncareacademy.com]

A Society concern:
- 1 in 5 hospitalised patients in European hospitals [Vanderwee et al., 2007]

Context

Pressure ulcers:

- Localized injury
- Long terme and/or excessive loading [Bouten et al., 2003]

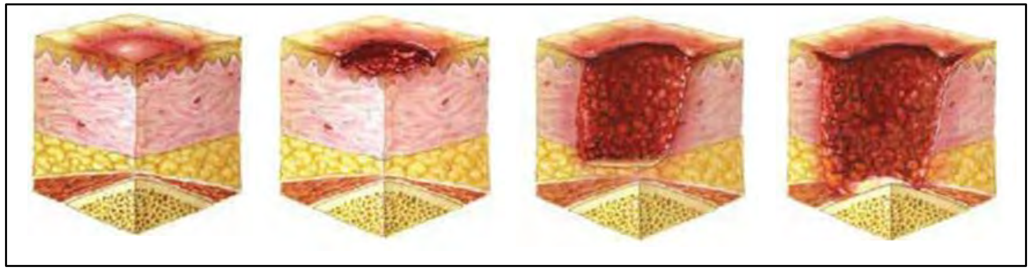

Stages 1 to 4 of pressure ulcers

[winncareacademy.com]

A Society concern:

- 1 in 5 hospitalised patients in European hospitals
  [Vanderwee et al., 2007]

Why?

- Lack of information to evaluate first signs: visual identification

Aetiology

Two major processes competing:

Ischaemia & reperfusion

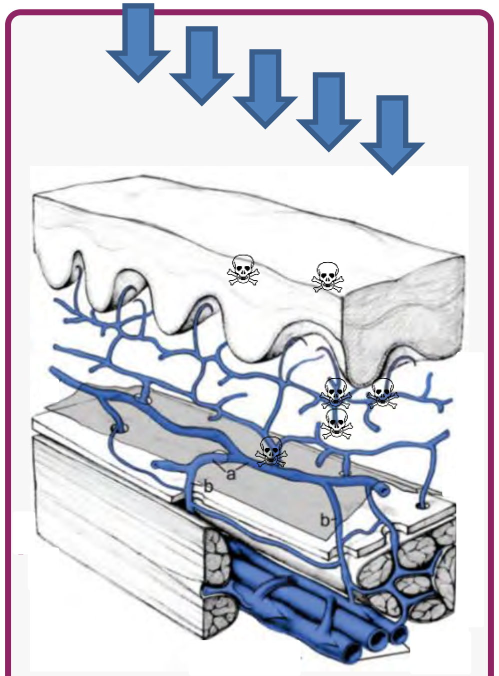

[Kosiak et al., 1959]
[Daniel et al., 1982]
[Landis,1930]

Aetiology

Two major processes competing:

Ischaemia & reperfusion

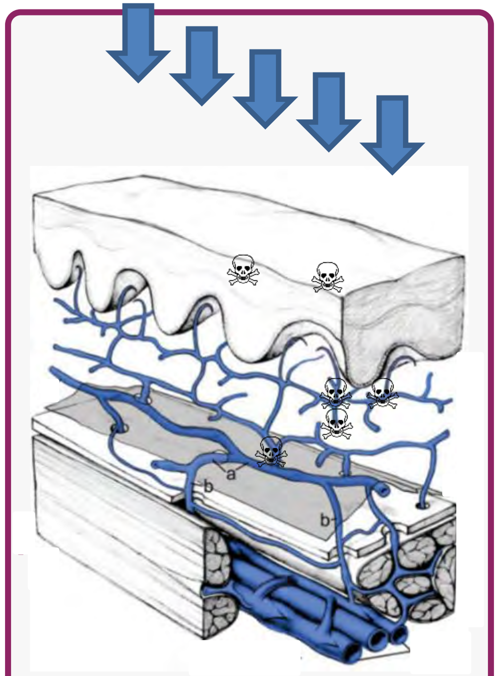

[Kosiak et al., 1959]
[Daniel et al., 1982]
[Landis,1930]

Deformation

Tissue damage threshold

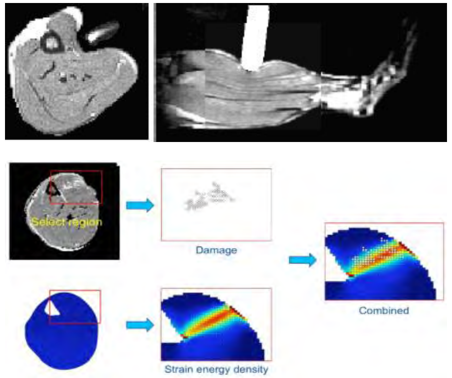

Animal Studies

[Ceelen et al., 2008]: (**N=11**)
[Traa 2019]: (**N=39**)
[Nelissen 2018]: (**N=53**)
[Nelissen 2017]: (**N=20**)
[Stekelenburg 2005]: (**N=10**)

Primary lesion-inducing factor

Mechanical aspect

How to model the soft tissue?

Challenge:

- Model the time dependent and loading history dependant behaviour
- Choice of a right material model for the soft tissue (type, structure…)

Existing material models of muscle

Authors	Year	Human/Animal	Samples	Confined Compression (CC) Unconfined Compression (UC)	Material Law
[Bosboom et al., 2001]	2001	Animal	In Vivo (n=4)	CC	Visco-hyper-elastic
[Aimedieu et al., 2003]	2003	Animal	Cylinders (n=6)	CC	Visco-elastic
[Van Loocke et al., 2006]	2006	Animal	Cuboids (n=12)	UC	Hyper-elastic
[Linder-Ganz et al., 2006]	2006	Human	In vivo (n=6)	CC	Visco-hyper-elastic
[Van Loocke et al., 2008]	2008	Animal	Cuboids (n=6)	UC	Visco-elastic
[Van Loocke et al., 2009]	2009	Animal	Cuboids	UC	Visco-hyper-elastic
[Wheatley et al., 2015]	2015	Animal	Cylinders (n=13 transverse & 13 longitudinal)	UC	Visco-hyper-elastic
[Vaidya and Wheatley, 2020]	2020	Animal	Cuboids (n=15 + 14) & Cylinders (n=16+15)	UC (Fast + Slow) & CC (Fast + Slow)	Visco-hyper-elastic

Existing material models of muscle

Authors	Year	Human/Animal	Samples	Confined Compression (CC) Unconfined Compression (UC)	Material Law
[Oomens et al., 1987]	1987	-	-	-	Theoritical Poroelastic Strain dependant permeability
[Argoubi and Shirazi-Adl, 1996]	1996	Human	-	-	Nonlinear poroelastic
[Bosboom et al., 2001]	2001	Animal	In Vivo (n=4)	CC	Visco-hyper-elastic
[Aimedieu et al., 2003]	2003	Animal	Cylinders (n=6)	CC	Visco-elastic
[Van Loocke et al., 2006]	2006	Animal	Cuboids (n=12)	UC	Hyper-elastic
[Linder-Ganz et al., 2006]	2006	Human	In vivo (n=6)	CC	Visco-hyper-elastic
[Van Loocke et al., 2008]	2008	Animal	Cuboids (n=6)	UC	Visco-elastic
[Van Loocke et al., 2009]	2009	Animal	Cuboids	UC	Visco-hyper-elastic
[Wheatley et al., 2015]	2015	Animal	Cylinders (n=13 transverse & 13 longitudinal)	UC	Visco-hyper-elastic
[Wheatley et al., 2016]	2016	Animal	Cylinders (n=4) Cuboid for model	UC	Poroelastic Moonley-Rivlin coupled model
[Vaidya and Wheatley, 2020]	2020	Animal	Cuboids (n=15 + 14) & Cylinders (n=16+15)	UC (Fast + Slow) & CC (Fast + Slow)	Visco-hyper-elastic

Existing material models of muscle

Muscle = Bi-phasic (up to 75% liquid)

[Wheatley et al., 2016]

Pores filled with Fluids

Solid

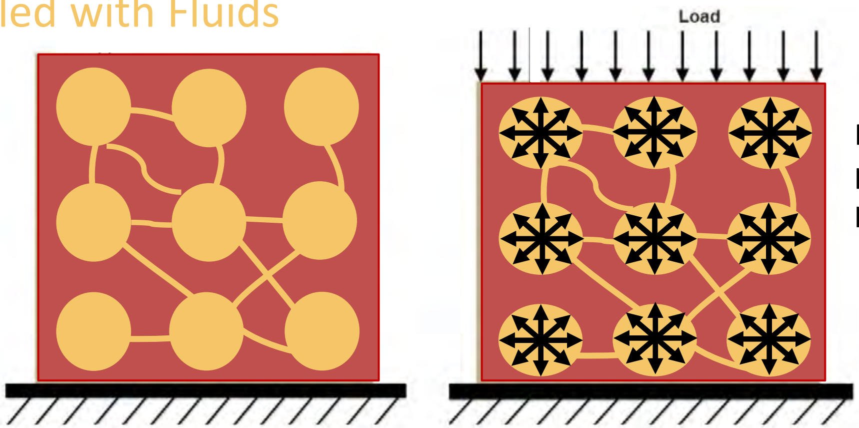

Increasing pore pressure

Existing material models of muscle

In vivo Boundary Conditions: Semi-confined

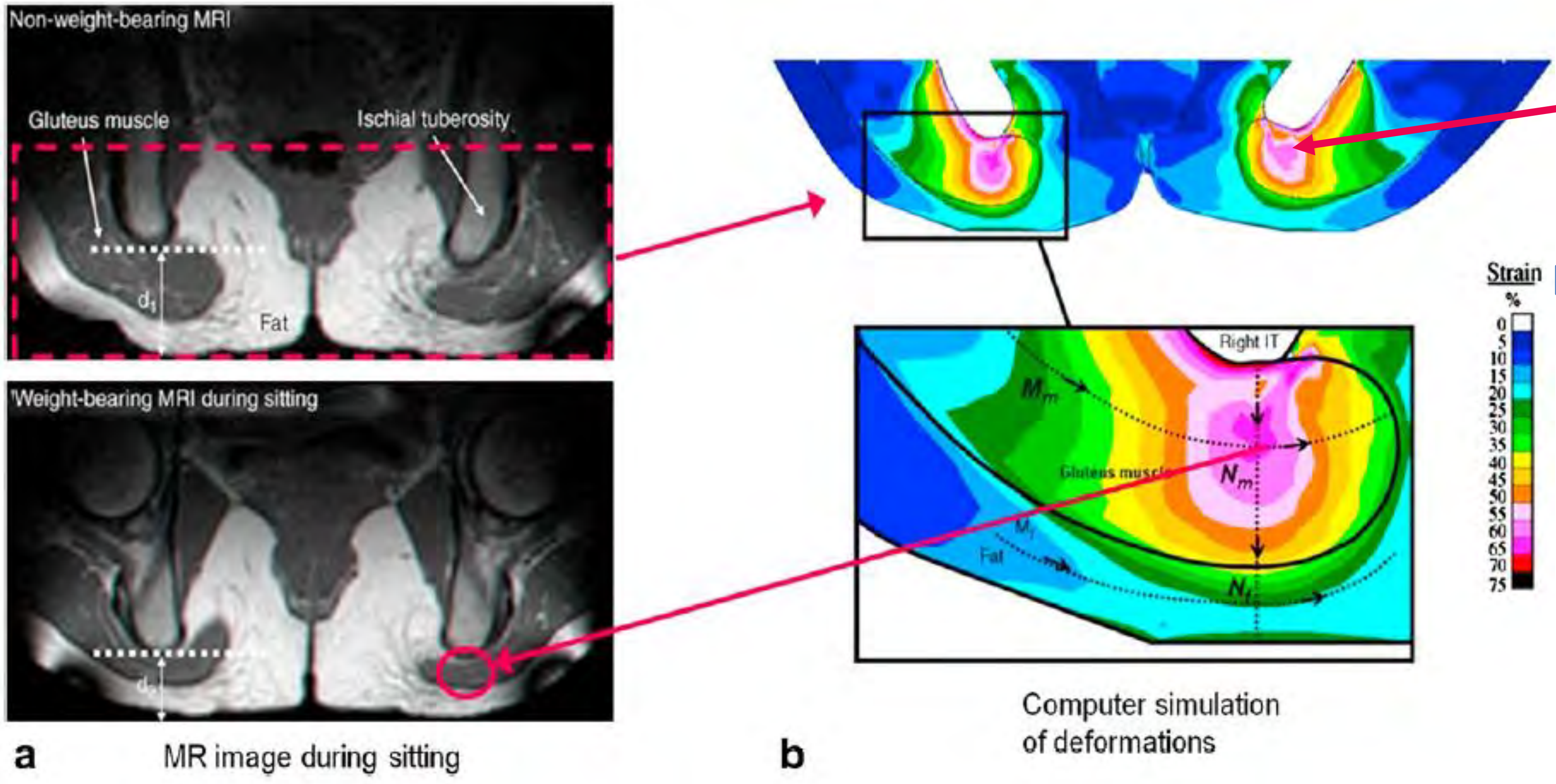

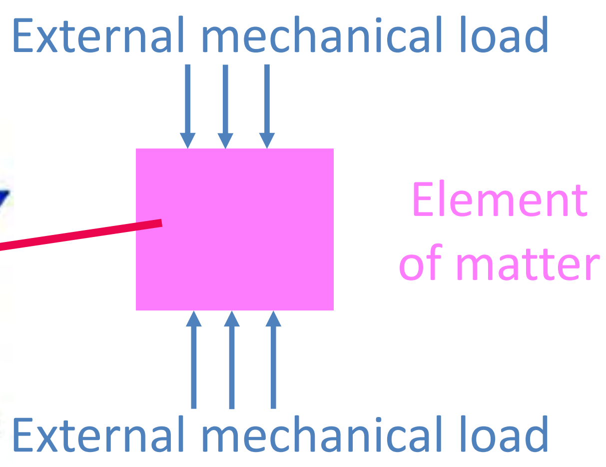

[Linder-Ganz et al., 2007]

Previous Study

An experimental and computational investigation of the effects of volumetric boundary conditions on the compressive mechanics of passive skeletal muscle

[Vaidya and Wheatley, 2020]

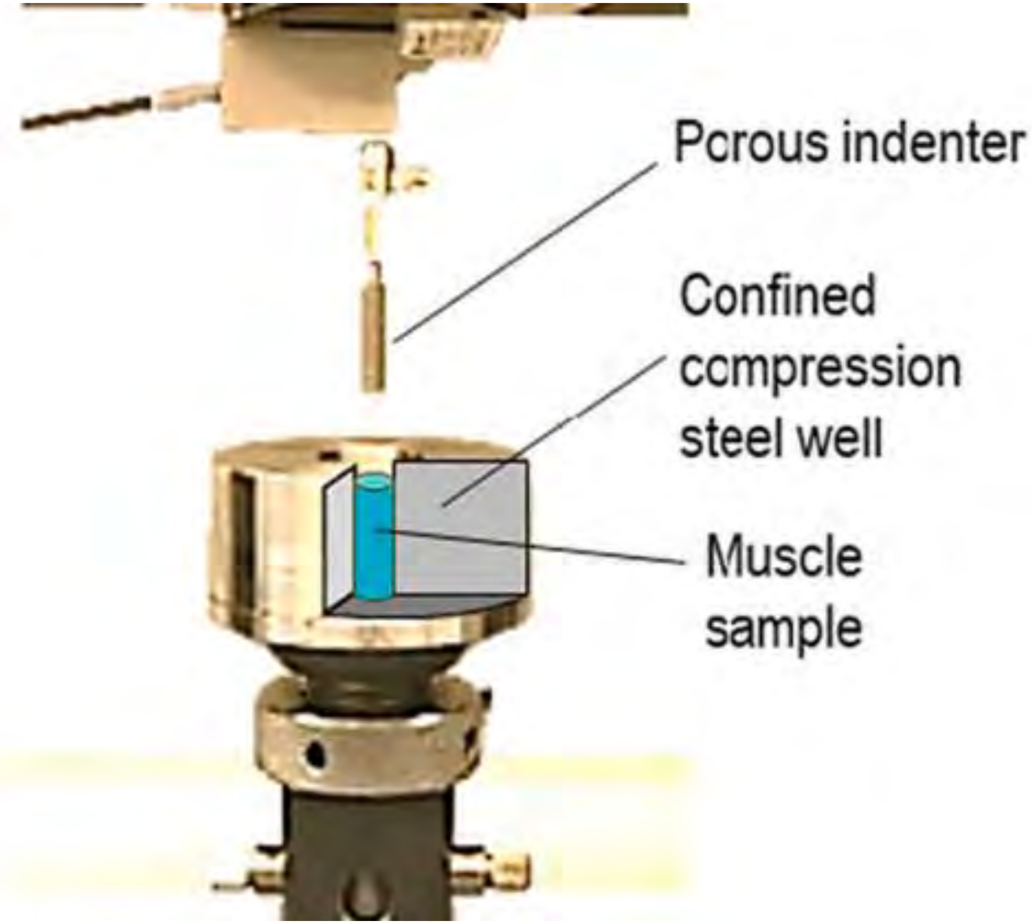

Final strain: 0.15

Fast strain rate: 0.15 s-1

N=16

Slow strain rate: 0.015 s-1

N=15

Objective

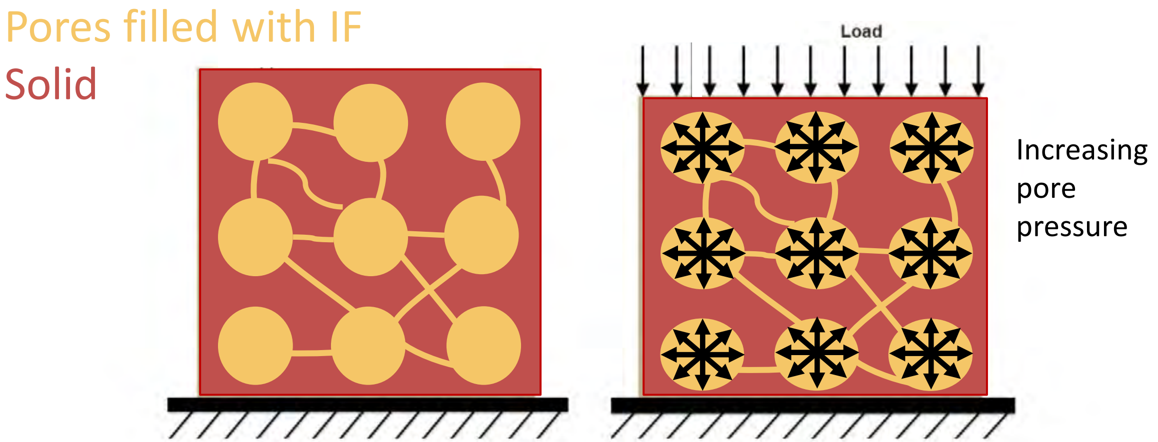

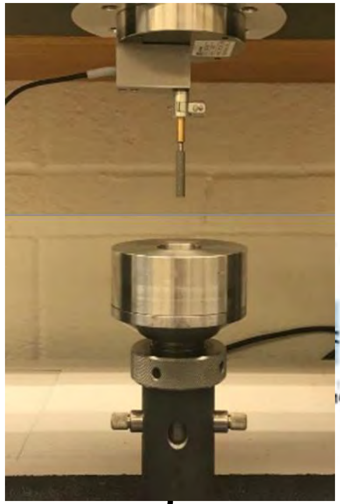

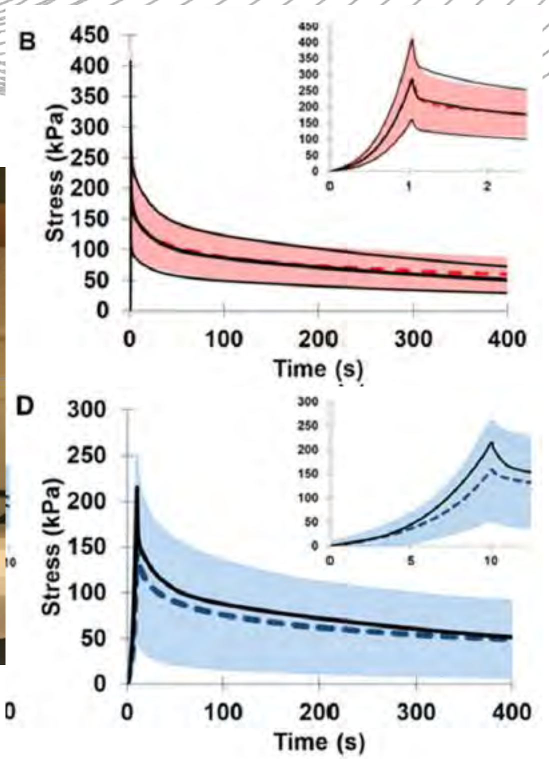

The possible role of poro-elasticity in the apparent visco-elastic behavior of passive muscle tissue under compression

- N=31 confined porcine muscle samples

Porous medium mechanics

Unknowns of the problem: $\boldsymbol{v}^s, p$

Pores filled with Fluids

Solid

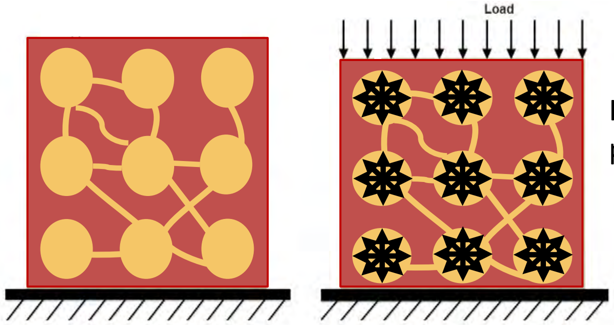

$$\begin{cases} \varepsilon^\alpha = \dfrac{Volume^\alpha}{Volume^{total}} \\ \varepsilon^s + \varepsilon^l = 1 \end{cases}$$

2 phases

Porous medium mechanics

Unknowns of the problem: $\boldsymbol{v}^{\boldsymbol{s}}, p$

Pores filled with Fluids

Solid

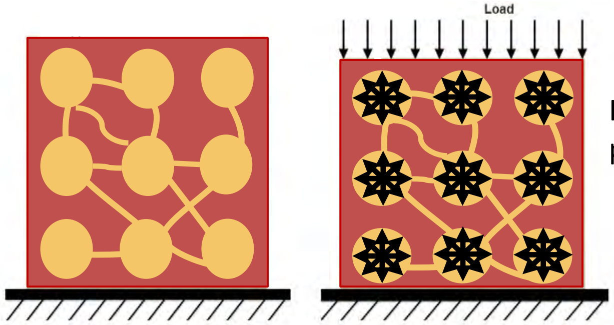

$$\begin{cases} \varepsilon^{\alpha} = \dfrac{Volume^{\alpha}}{Volume^{total}} \\ \varepsilon^{s} + \varepsilon^{l} = 1 \end{cases}$$ 2 phases

$$\varepsilon^{l}(\boldsymbol{v}^{\boldsymbol{l}} - \boldsymbol{v}^{\boldsymbol{s}}) = -\frac{k^{\varepsilon}}{\mu^{l}}(\boldsymbol{\nabla} p - \rho^{l}\boldsymbol{g})$$ Fluid Phase: Darcy's law

Porous medium mechanics

Unknowns of the problem: $\boldsymbol{v^s}, p$

Pores filled with Fluids

Solid

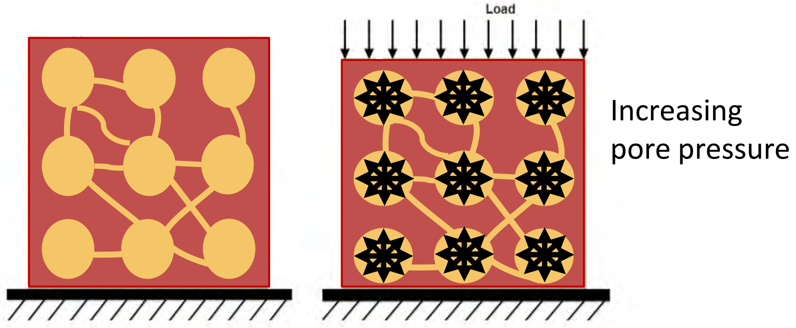

$$\begin{cases} \varepsilon^{\alpha} = \dfrac{Volume^{\alpha}}{Volume^{total}} \\ \varepsilon^{s} + \varepsilon^{l} = 1 \end{cases}$$

2 phases

$$\boldsymbol{t^{total}} = \varepsilon^{s}\boldsymbol{t^s} + \varepsilon^{l}\boldsymbol{t^l} = \boldsymbol{t^{eff}} - \beta p\, \boldsymbol{I}_d$$

Stress tensor as a combination of the solid scaffold stress and pore pressure

Porous medium mechanics

Unknowns of the problem: $\boldsymbol{v}^{\boldsymbol{s}}, p$

$$
\begin{cases}
\dfrac{D^s}{Dt}(\rho^s \varepsilon^s) + \rho^s \varepsilon^s \nabla \cdot \boldsymbol{v}^{\boldsymbol{s}} = 0 \\
\dfrac{D^s}{Dt}(\rho^l \varepsilon^l) + \nabla \cdot (\rho^l \varepsilon^l (\boldsymbol{v}^{\boldsymbol{l}} - \boldsymbol{v}^{\boldsymbol{s}})) + \rho^l \varepsilon^l \nabla \cdot \boldsymbol{v}^{\boldsymbol{s}} = 0 \\
\nabla \cdot (\boldsymbol{t}^{\boldsymbol{tot}}) + \boldsymbol{f}_{\boldsymbol{v}} = \rho^s \boldsymbol{\gamma}^{\boldsymbol{s}}
\end{cases}
$$

Solid Scaffold: Mass balance

Fluid Phase: Mass balance

Momentum balance

FEM model

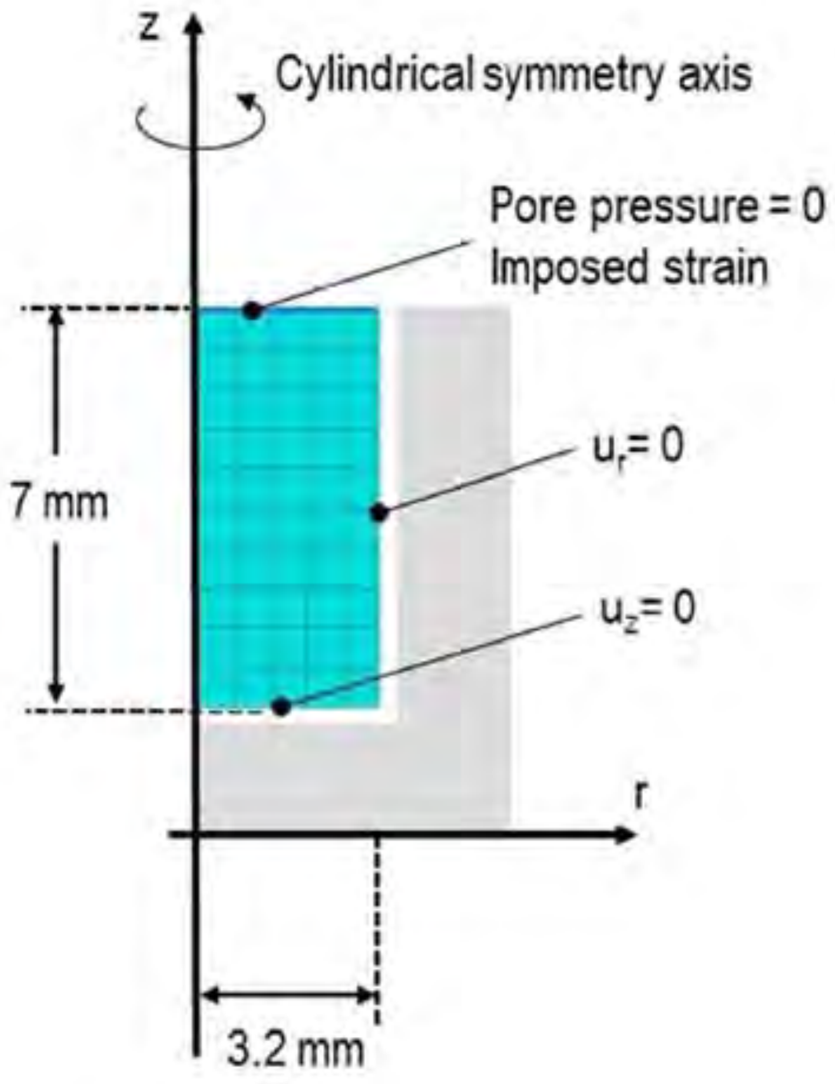

- n=50 (P2,P1) Taylor Hood elements
- Fluid leakage on top surface
- Bottom and lateral displacement fixed

FEM model

Material law based on 6 parameters: Poro-elasticity

Solid Phase			Fluid Phase		
Linear Elasticity		Soil Grain Bulk Modulus	Darcy's Law		Fluid Bulk Modulus
E (kPa)	ν (-)	K^s (MPa)	$k\ (m^2 Pa^{-1} s^{-1})$	Void Ratio (-)	K^l (MPa)

Fixed parameters: 0.4879, 0.799, 2200

FEM model

Material law based on 6 parameters: Poro-elasticity

Solid Phase			Fluid Phase		
Linear Elasticity		Soil Grain Bulk Modulus	Darcy's Law		Fluid Bulk Modulus
E (kPa)	ν (-)	K^s (MPa)	$k\ (m^2Pa^{-1}s^{-1})$	Void Ratio (-)	K^l (MPa)

Calibrated parameters

Cost function

X=[Young's modulus, Hydraulic permeability, Void ratio]

Peak Stress

$$J_1 = \frac{1}{3} * (\frac{\max(\mathbf{t}^{tot}_{abq}) - \max(\mathbf{t}^{tot}_{exp})}{\max(\mathbf{t}^{tot}_{exp})})^2$$

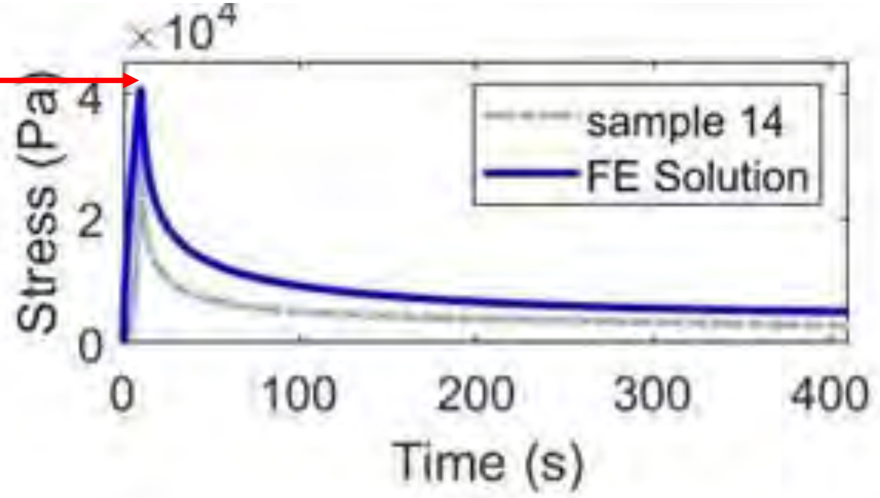

Cost function

X=[Young's modulus, Hydraulic permeability, Void ratio]

Peak Stress

$$J_1 = \frac{1}{3} * \left(\frac{\max(\mathbf{t}_{abq}^{tot}) - \max(\mathbf{t}_{exp}^{tot})}{\max(\mathbf{t}_{exp}^{tot})}\right)^2$$

Slope at the end

$$J_2 = \frac{1}{3} * \left(\frac{\frac{\partial \mathbf{t}_{abq}^{tot}}{\partial t} - \frac{\partial \mathbf{t}_{exp}^{tot}}{\partial t}}{\frac{\partial \mathbf{t}_{exp}^{tot}}{\partial t}}\right)^2$$

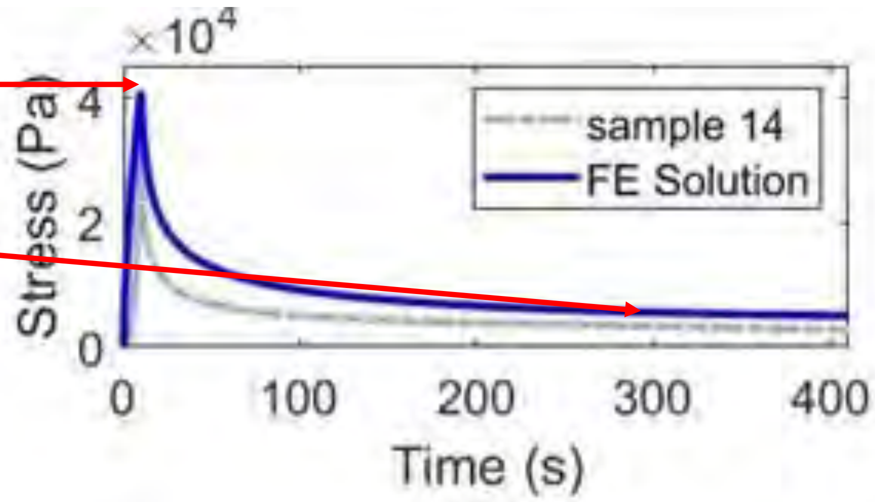

Cost function

X=[Young's modulus, Hydraulic permeability, Void ratio]

Peak Stress

$$J_1 = \frac{1}{3} * \left(\frac{\max(\mathbf{t}^{tot}_{abq}) - \max(\mathbf{t}^{tot}_{exp})}{\max(\mathbf{t}^{tot}_{exp})}\right)^2$$

Slope at the end

$$J_2 = \frac{1}{3} * \left(\frac{\frac{\partial \mathbf{t}^{tot}_{abq}}{\partial t} - \frac{\partial \mathbf{t}^{tot}_{exp}}{\partial t}}{\frac{\partial \mathbf{t}^{tot}_{exp}}{\partial t}}\right)^2$$

Normalised RMSE

$$J_3 = \frac{1}{3} * \left(\frac{rms(\mathbf{t}^{tot}_{abq} - \mathbf{t}^{tot}_{exp})}{norm(\mathbf{t}^{tot}_{exp})}\right)^2$$

Cost function

$$J = J_1 + J_2 + J_3$$

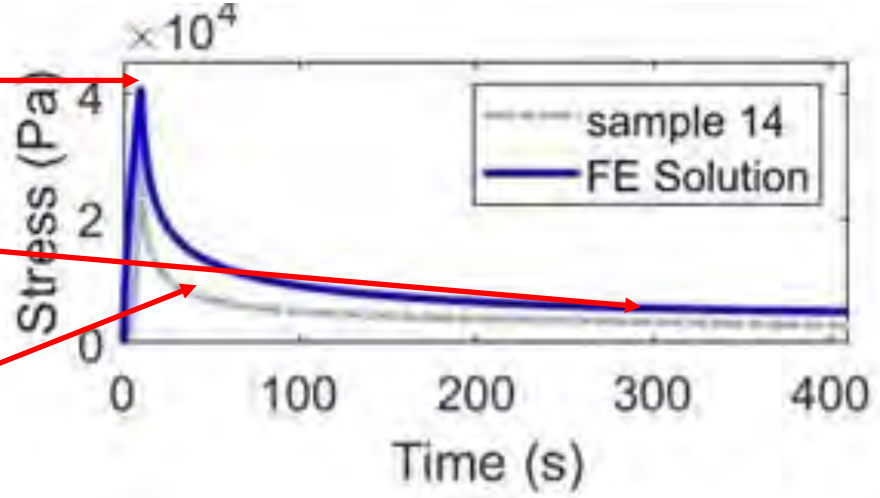

Results

1 to 1 calibration (N=15 slow et N=16 fast)

Slow strain-rate: Average

Fast strain-rate: Average

Results

Slow strain-rate: Average

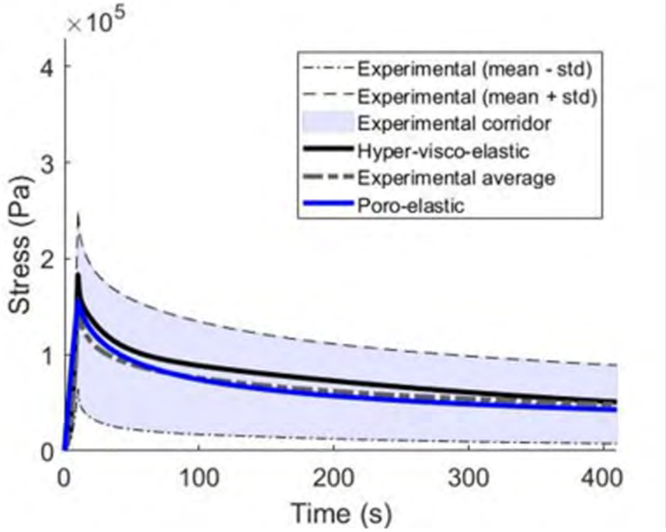

Model	Strain-rate	Peak-stress error (J1)	End Slope error (J2)	Area between the curves (J3)	Cost function (J)
Uncoupled Yeoh/Prony visco-hyper-elastic [Vaidya and Wheatley, 2020]	Slow	0.0283	0.5936	0.0081	0.21
	Fast				
Poro-linear-elastic Current study	Slow	0.00005	0.00079	0.0039	0.0016
	Fast				

Results

Slow strain-rate: Average

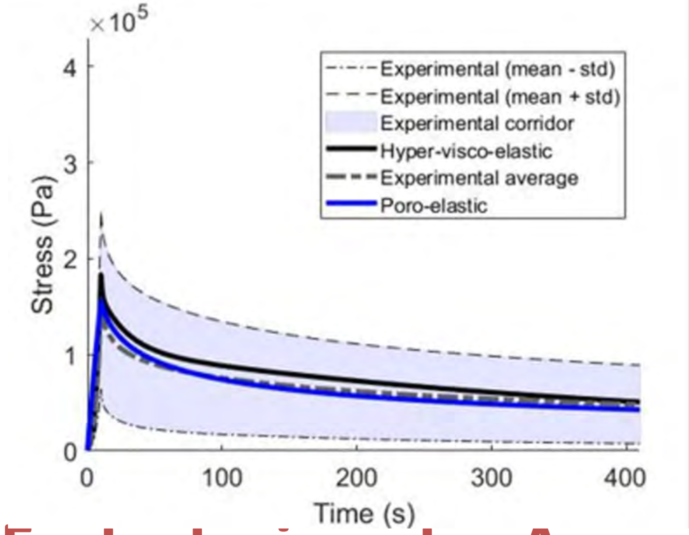

Fast strain-rate: Average

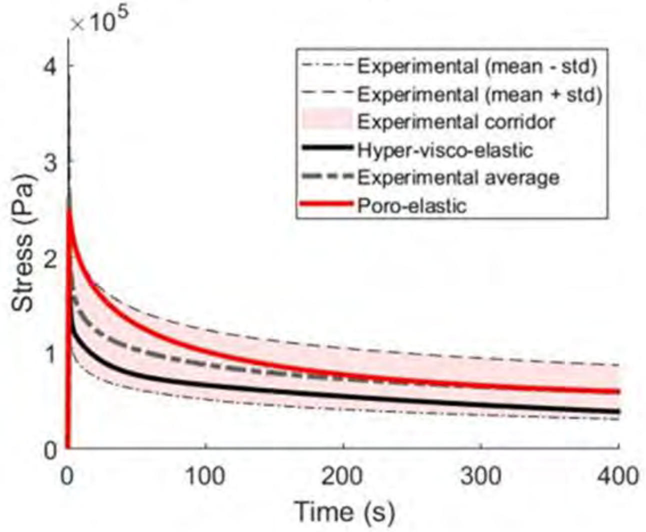

Model	Strain-rate	Peak-stress error (J1)	End Slope error (J2)	Area between the curves (J3)	Cost function (J)
Uncoupled Yeoh/Prony visco-hyper-elastic [Vaidya and Wheatley, 2020]	Slow	0.0283	0.5936	0.0081	0.21
	Fast	0.1559	0.4611	0.0046	0.2477
Poro-linear-elastic Current study	Slow	0.00005	0.00079	0.0039	0.0016
	Fast	0.0026	0.0092	0.007	0.0061

Discussion [Vaidya and Wheatley, 2020]

Final strain: 0.15
Fast strain rate: 0.15 s-1

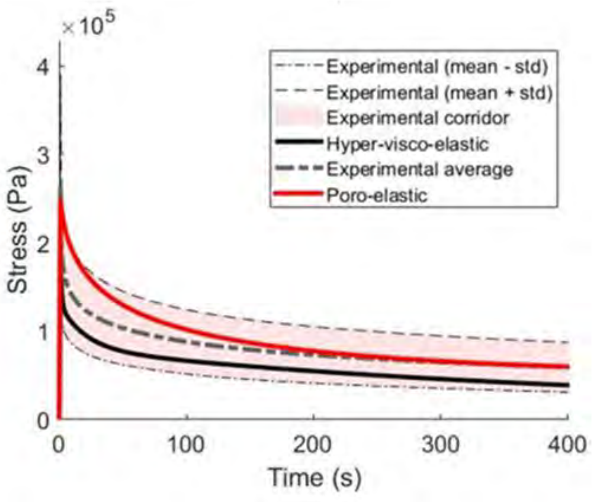

Final strain: 0.15
Slow strain rate: 0.015 s-1

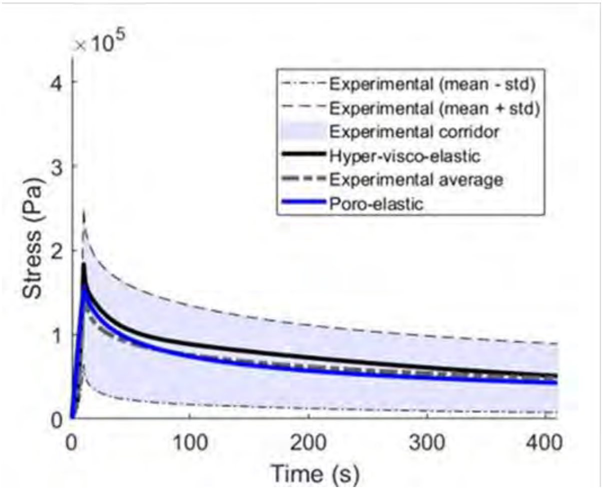

Previously: [Vaidya and Wheatley, 2020]

Material = Yeoh Hyper-elasticity coupled with Prony Series
=>18 calibrated parameters

Discussion [Vaidya and Wheatley, 2020]

Final strain: 0.15
Fast strain rate: 0.15 s-1

Final strain: 0.15
Slow strain rate: 0.015 s-1

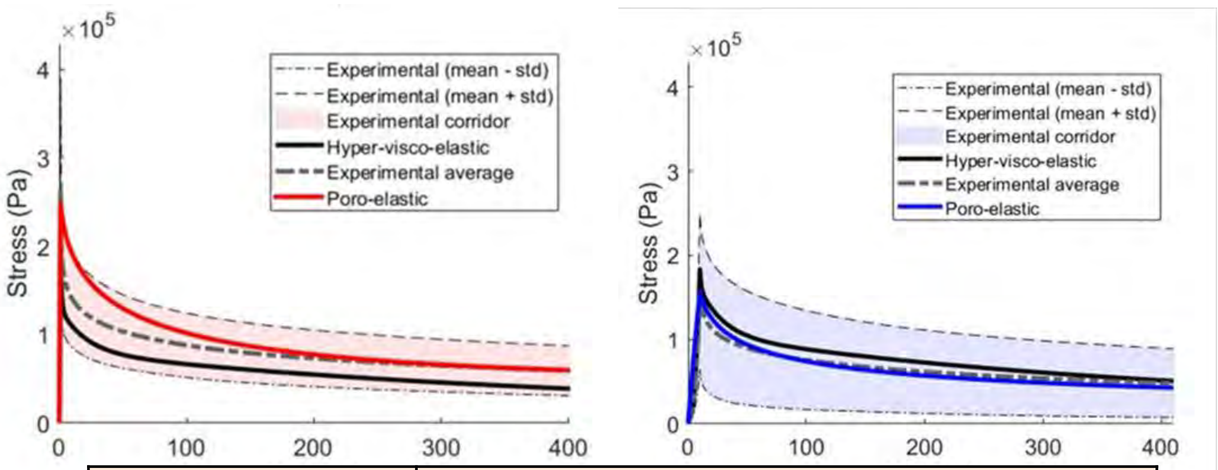

Solid Phase	Fluid Phase	
Young's Modulus (kPa)	Hydraulic permeability ($m^2Pa^{-1}s^{-1}$)	Void ratio (-)
12.89 ± 11.29	$(2.09 \pm 3.12) \times 10^{-13}$	0.469 ± 0.247
20.16 ± 8.54	$(1.94 \pm 5.71) \times 10^{-13}$	0.640 ± 0.325

Previously: [Vaidya and Wheatley, 2020]

Material = Yeoh Hyper-elasticity coupled with Prony Series
=>18 calibrated parameters

This Study :

Bi-phasic Material = Poro-linear-elasticity
=> 4 fixed parameters and 3 calibrated parameters

Discussion: Are the parameters relevant?

Solid Phase:

Young's Modulus E (kPa): [Gras et al., 2012a ; Gras et al., 2012b ; Palevski et al., 2006]

$$2.4 < E = 16 \pm 10 < 1860$$

✓

Discussion: Are the parameters relevant?

Solid Phase:

Young's Modulus E (kPa): [Gras et al., 2012a ; Gras et al., 2012b ; Palevski et al., 2006]

$$2.4 < E = 16 \pm 10 < 1860$$

Fluid Phase:

Hydraulic Permeability k ($m^2Pa^{-1}s^{-1}$): [Wheatley et al., 2016 ; Gimnich et al., 2019]

$$4 \times 1e-14 < k = (2 \pm 4) \times 1e-13 < 1 \times 1e-9$$

Discussion: Are the parameters relevant?

Solid Phase:

Young's Modulus E (kPa): [Gras et al., 2012a ; Gras et al., 2012b ; Palevski et al., 2006]

$$2.4 < E = 16 \pm 10 < 1860$$ ✓

Fluid Phase:

Hydraulic Permeability k ($m^2Pa^{-1}s^{-1}$): [Wheatley et al., 2016 ; Gimnich et al., 2019]

$$4 \times 1e - 14 < k = (2 \pm 4) \times 1e - 13 < 1 \times 1e - 9$$ ✓

Void Ratio e (-): [Argoubi and Shirazi-Adl, 1996]

$e \in [0.1 ; 0.3]$ for bones and cartilage

$e = (0.6 \pm 0.3)$ ✓

Discussion: Limits of the model

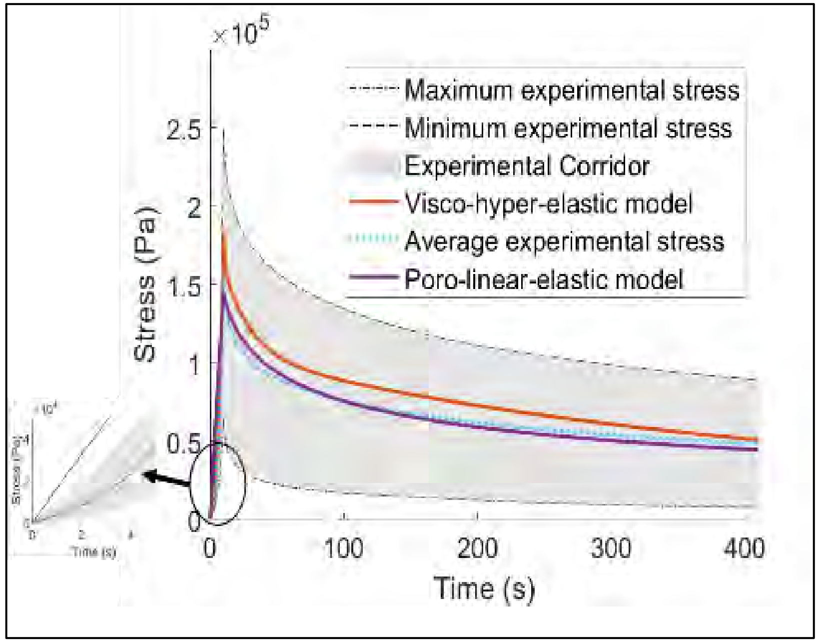

Error on the initial slope :

- Linear behaviour of the laws ?
- Experimental error ?

Discussion: Limits of the model

Initial Guess			Cost Function
E (Pa)	k ($m^2Pa^{-1}s^{-1}$)	Void Ratio (-)	J
17989	0.6996	6.07×10^{-14}	0.0061
8995	0.3498	3.035×10^{-14}	0.0084

Minimization based on the gradients
=> risk of local minimums

Strong interplay between the Young's modulus and the hydraulic permeability

Discussion: Limits of the model

Initial Guess			Cost Function
E (Pa)	k $(m^2Pa^{-1}s^{-1})$	Void Ratio (-)	J
17989	0.6996	6.07×10^{-14}	0.0061
8995	0.3498	3.035×10^{-14}	0.0084

Experimental determination of some parameters would avoid these potential local minimums [Fougeron et al., 2020]

Elastography

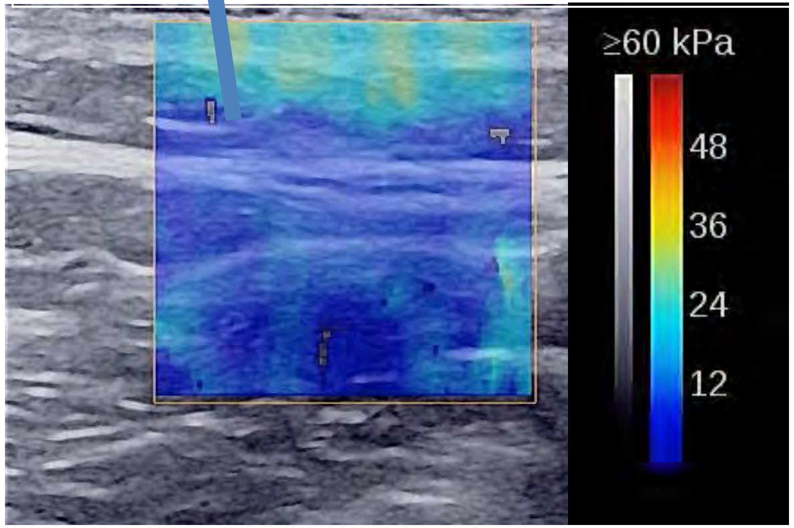

Power doppler

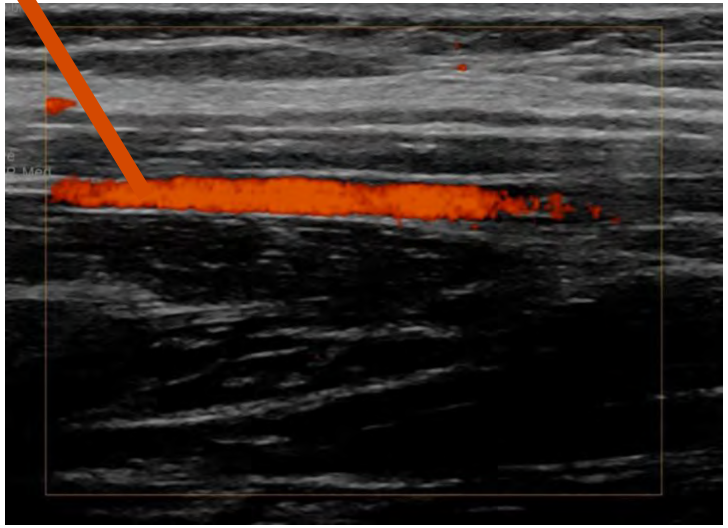

Conclusion and perspectives

Modelling the apparent viscoelastic behaviour of passive muscle tissue under confined compression using a poroelastic framework

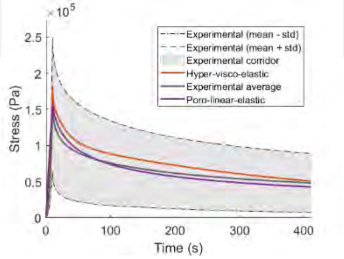

- Peak stress and relaxation behaviour mostly recovered

Conclusion and perspectives

Modelling the apparent viscoelastic behaviour of passive muscle tissue under confined compression using a poroelastic framework

- Peak stress and relaxation behaviour mostly recovered

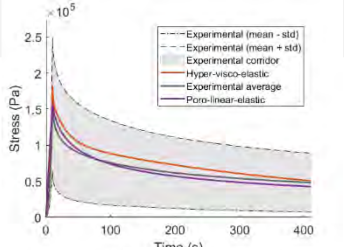

- Respect the structural architecture of the muscle

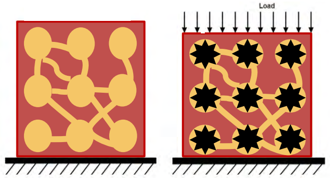

Conclusion and perspectives

Modelling the apparent viscoelastic behaviour of passive muscle tissue under confined compression using a poroelastic framework

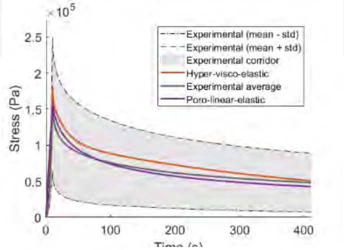

- Peak stress and relaxation behaviour mostly recovered

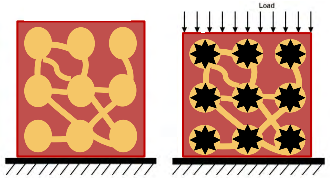

Increasing pore pressure

- Respect the structural architecture of the muscle

- Only 6 parameters & possibility to evaluate them experimentally

Solid Phase			Fluid Phase			
Linear Elastic Law		Soil Grain Bulk Modulus	Darcy's Law			Fluid Bulk Modulus
E (kPa)	ν (-)	K^s (MPa)	k ($m^2\,Pa^{-1}\,s^{-1}$)	Dynamic Viscosity (Pa s)	Void ratio (-)	K^l (MPa)

Conclusion and perspectives

Modelling the apparent viscoelastic behaviour of passive muscle tissue under confined compression using a poroelastic framework

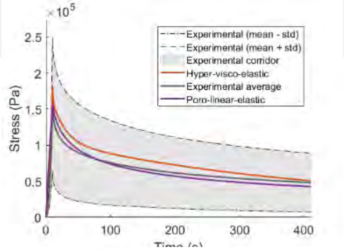

- Peak stress and relaxation behaviour mostly recovered

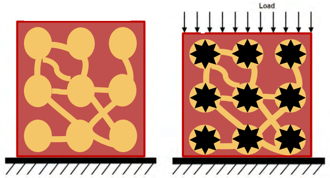

- Respect the structural architecture of the muscle
- Only 6 parameters & possibility to evaluate them experimentally

Solid Phase			Fluid Phase			
Linear Elastic Law		Soil Grain Bulk Modulus	Darcy's Law			Fluid Bulk Modulus
E (kPa)	ν (-)	K^s (MPa)	k ($m^2\,Pa^{-1}\,s^{-1}$)	Dynamic Viscosity (Pa s)	Void ratio (-)	K^l (MPa)

- Possibility to go towards a multiscale/multiphasic model: biomarkers & inflammatory signaling pathways

[Sciumè, 2021]
[Sciume *et al.*, 2013]
[Urcun et al., 2020]

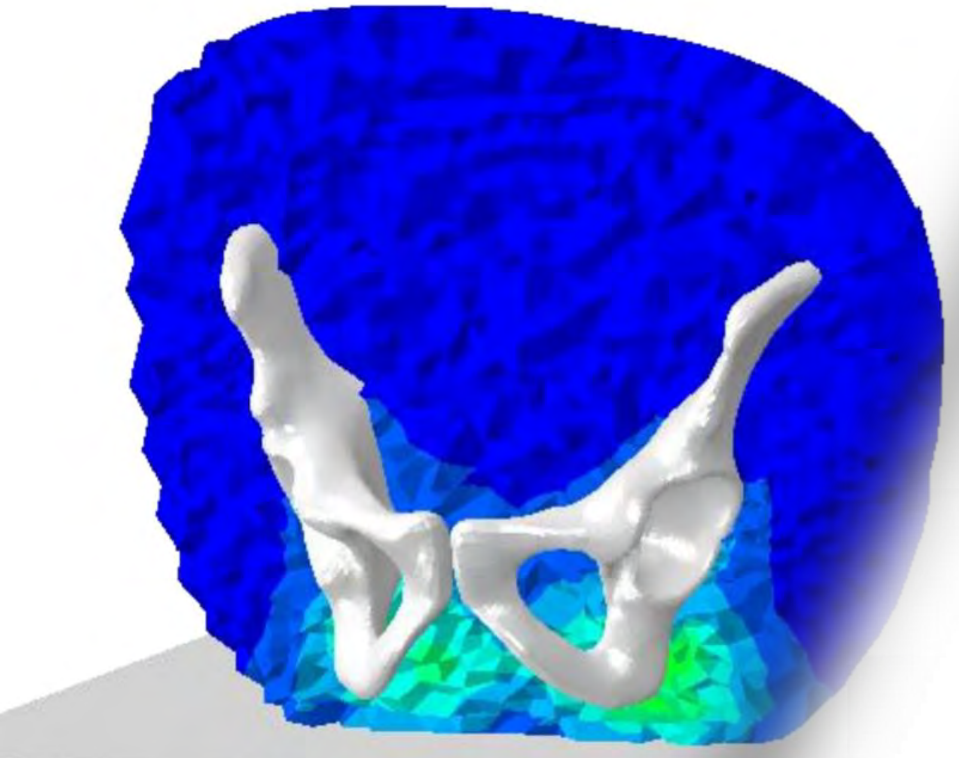

[Macron et al., 2018]

Thank you for your attention!

Do you have any questions?

Corresponding author: thomas.lavigne@ext.uni.lu

Bibliography

[Macron et al., 2018]: Development and evaluation of a new methodology for the fast generation of patient-specific finite element models of the buttock for sitting-acquired deep tissue injury prevention
[Bouten et al., 2003]: The etiology of pressure ulcers: Skin deep or muscle bound?
[Vanderwee et al., 2007]: Pressure ulcer prevalence in Europe: a pilot study
[Kosiak et al., 1959]: Etiology and pathology of ischemic ulcers
[Ceelen et al., 2008]: Compression-induced damage and internal tissue strains are related
[Linder Ganz et al., 2006]: Pressure-time cell death threshold for albino rat skeletal muscles as related to pressure sore biomechanics
[Loerakker et al., 2011]: The effects of deformation, ischemia, and reperfusion on the development of muscle damage during prolonged loading
[Linder-Ganz et al., 2007]: Assessment of mechanical conditions in sub-dermal tissues during sitting: A combined experimental-MRI and finite element approach
[Landis,1930]: Micro-injection studies of capillary blood pressure in human skin
[Oomens et al., 1987]: A mixture approach to the mechanics of skin
[Argoubi and Shirazi-Adl, 1996]: Poroelastic creep response analysis of a lumbar motion segment in compression
[Bosboom et al., 2001]: Passive transverse mechanical properties of skeletal muscle under in vivo compression
[Aimedieu et al., 2003]: Dynamic stiffness and damping of porcine muscle specimens,
[Van Loocke et al., 2006]: A validated model of passive muscle in compression
[Van Loocke et al., 2008]: Viscoelastic properties of passive skeletal muscle in compression: Stress-relaxation behaviour and constitutive modelling
[Van Loocke et al., 2009]: Viscoelastic properties of passive skeletal muscle in compression|cyclic behaviour
[Wheatley et al., 2015]: Fully non-linear hyper-viscoelastic modeling of skeletal muscle in compression
[Wheatley et al., 2016]: A case for poroelasticity in skeletal muscle – finite element analysis: experiment and modelling
[Vaidya and Wheatley, 2020]: An experimental and computational investigation of the effects of volumetric boundary conditions on the compressive mechanics of passive skeletal muscle
[Peyrounette et al., 2018]: Multiscale modelling of blood ow in cerebral microcirculation: Details at capillary scale control accuracy at the level of the cortex
[Gras et al., 2012a]: Hyper-elastic properties of the human sternocleidomastoideus muscle in tension
[Gras et al., 2012b]: The nonlinear response of a muscle in transverse compression: assessment of geometry influence using a finite element model
[Palevski et al., 2006]: Stress relaxation of porcine gluteus muscle subjected to sudden transverse deformation as related to pressure sore modeling
[Gimnich et al., 2019]: Magnetic resonance imaging based modeling of microvascular perfusion in patients with peripheral artery disease
[Fougeron et al., 2020]: Combining freehand ultrasound-based indentation and inverse finite element modeling for the identication of hyperelastic material properties of thigh soft tissues
[Sciume et al., 2013]: A multiphase model for three-dimensional tumor growth
[Urcun et al., 2020]: Digital twinning of cellular capsule technology: emerging outcomes from the perspective of porous media mechanics
[Sciumè, 2021]: Mechanistic modeling of vascular tumor growth: an extension of Biot's theory to hierarchical bi-compartment porous medium system
[Soltz and Ateshian, 1998]: Experimental verification and theoretical prediction of cartilage interstitial fluid pressurization at an impermeable contact interface in confined compression
[Ceelen 2008] Compression-induced damage and internal tissue strains are related
[Traa 2019] There is an individual tolerance to mechanical loading in compression induced deep tissue injury
[Nelissen 2018] An advanced magnetic resonance imaging perspective on the etiology of deep tissue injury
[Nelissen 2017] A MRI-Compatible Combined Mechanical Loading and MR Elastography Setup to Study Deformation-Induced Skeletal Muscle Damage in Rats
[Stekelenburg 2005] A new MR-compatible loading device to study in vivo muscle damage development in rats due to compressive loading

Appendix A: Almost incompressible model

(nu=0.4879)

Final strain: 0.15
Fast strain rate: 0.15 s-1

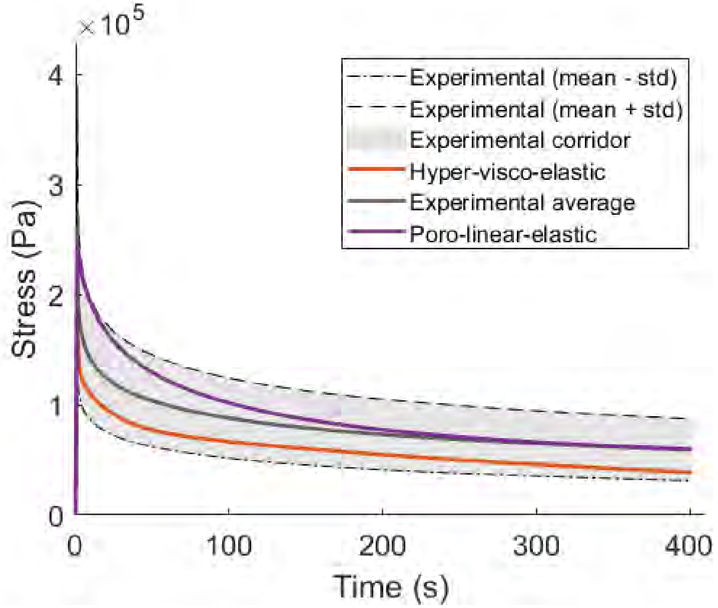

Final strain: 0.15
Slow strain rate: 0.015 s-1

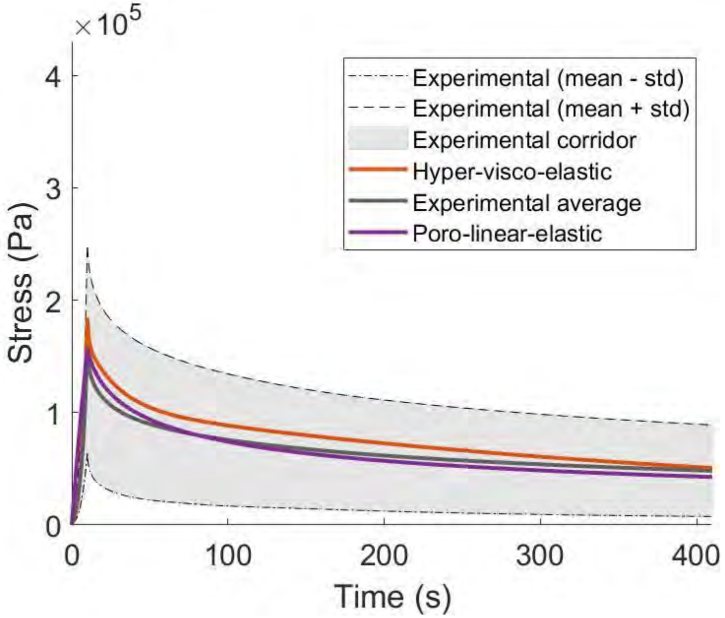

Solid Phase	Fluid Phase	
Young's Modulus (kPa)	Hydraulic permeability ($m^2Pa^{-1}s^{-1}$)	Void ratio (-)
12.89 ± 11.29	$(2.09 \pm 3.12) \times 10^{-13}$	0.469 ± 0.247
20.16 ± 8.54	$(1.94 \pm 5.71) \times 10^{-13}$	0.640 ± 0.325

Appendix A: Almost incompressible model

(nu=0.4879)

Slow strain-rate: N=15

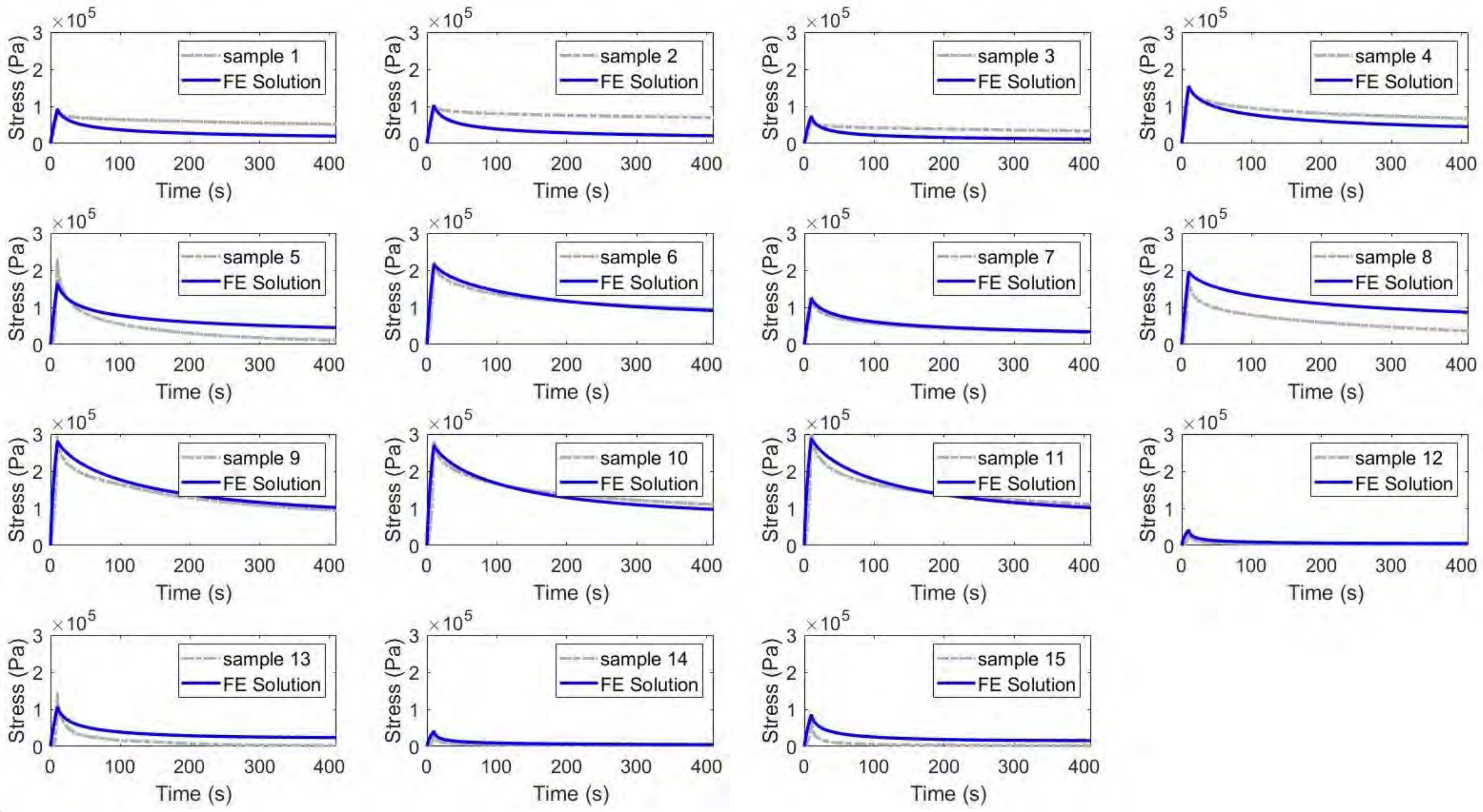

J: 0.0279±0.0461

Appendix A: Almost incompressible model

(nu=0.4879)

Fast strain-rate: N=16

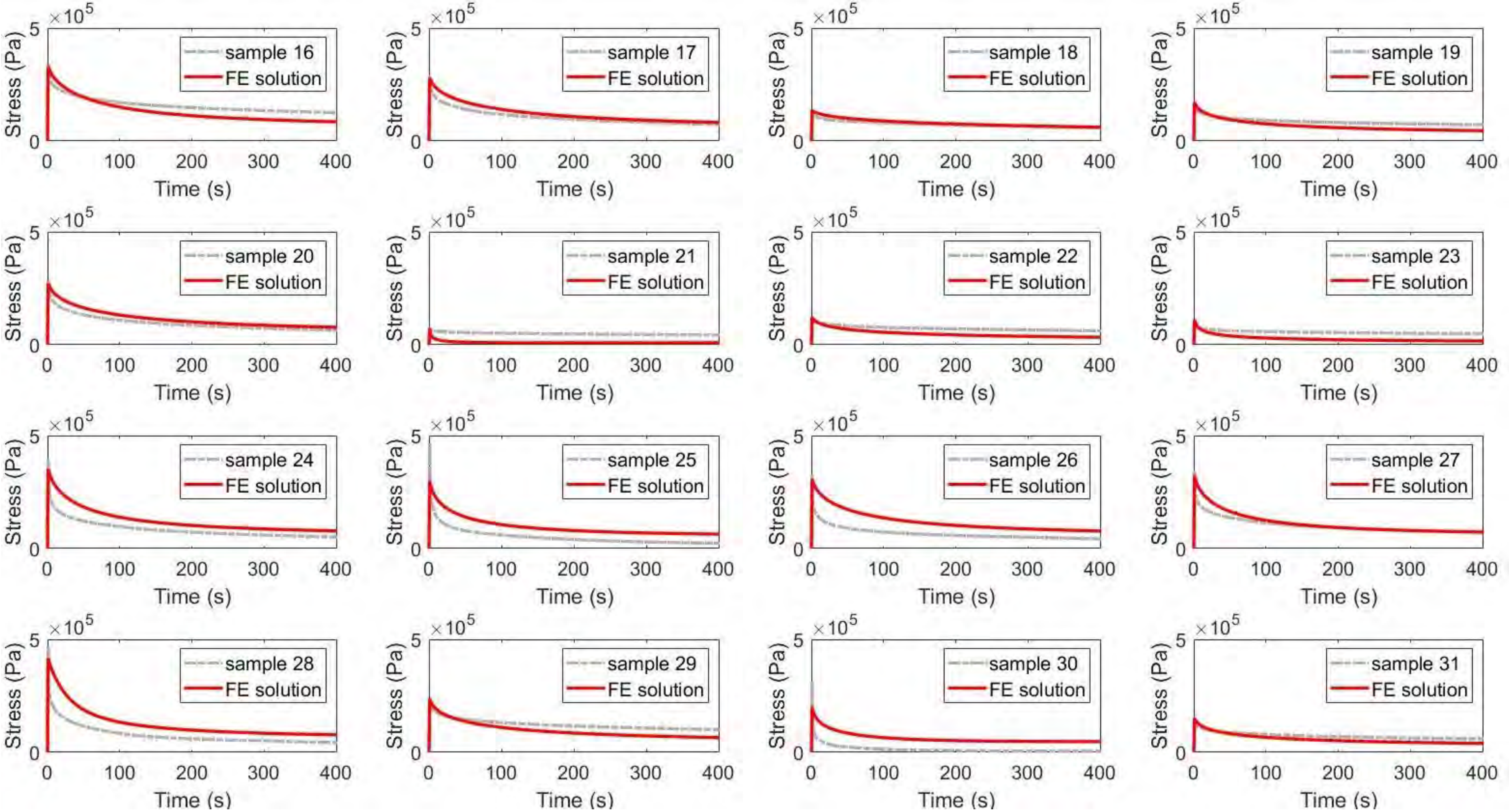

J: 0.0523±0.1094

Appendix B: Compressible model (nu=0.2)

Final strain: 0.15
Fast strain rate: 0.15 s-1

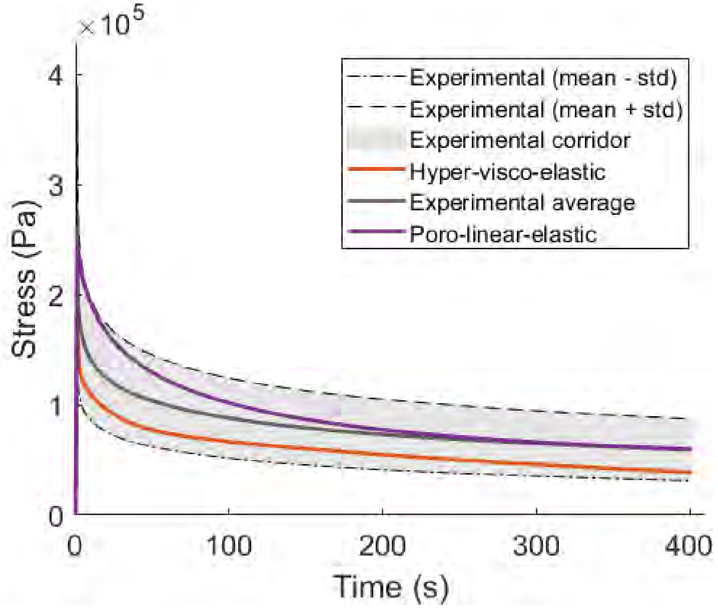

Final strain: 0.15
Slow strain rate: 0.015 s-1

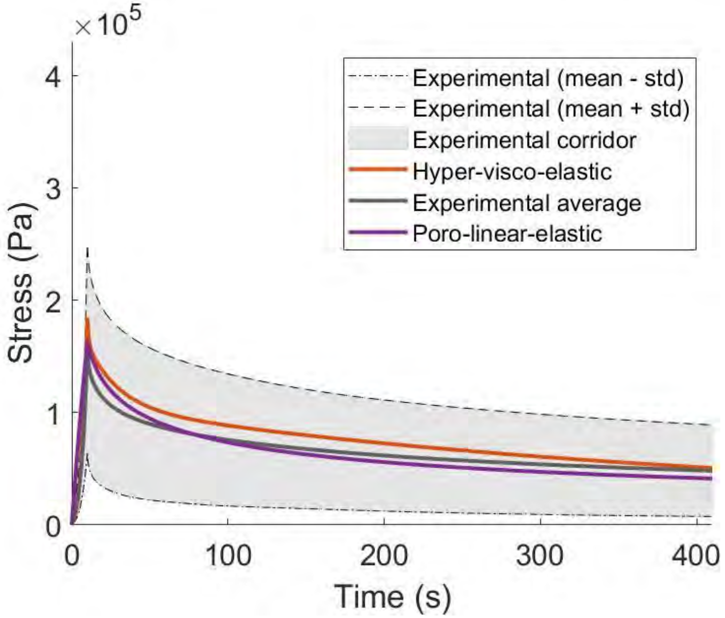

Solid Phase	Fluid Phase	
Young's Modulus (kPa)	Hydraulic permeability ($m^2 Pa^{-1} s^{-1}$)	Void ratio (-)
116.02 ± 31.89	$(1.16 \pm 1.93) \times 10^{-12}$	0.81 ± 0.24
133.75 ± 24.54	$(1.87 \pm 4.17) \times 10^{-12}$	0.95 ± 0.11

Appendix B: Compressible model (nu=0.2)

Slow strain-rate: N=15

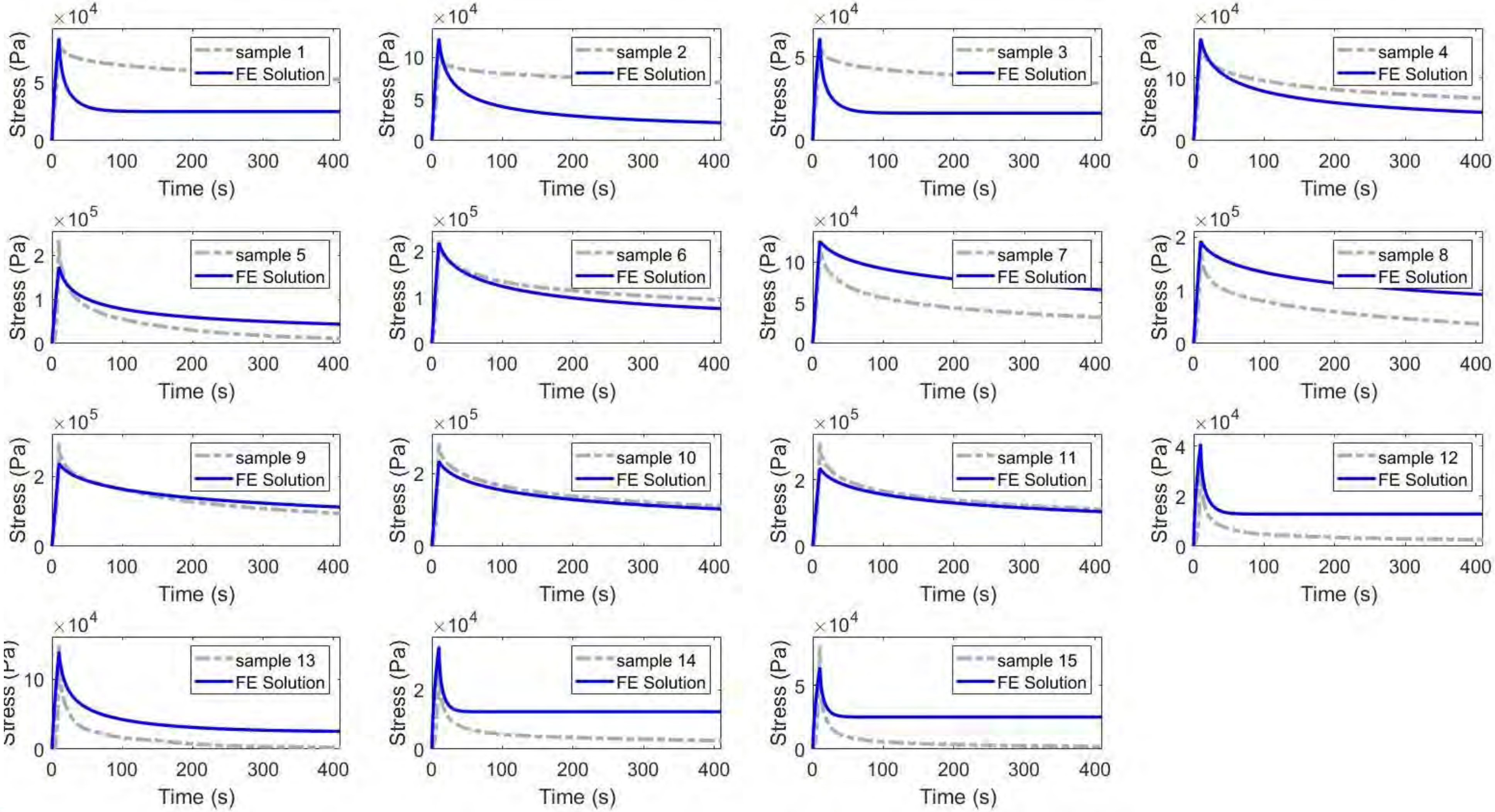

J: 0.121±0.161

Appendix B: Compressible model (nu=0.2)

Fast strain-rate: N=16

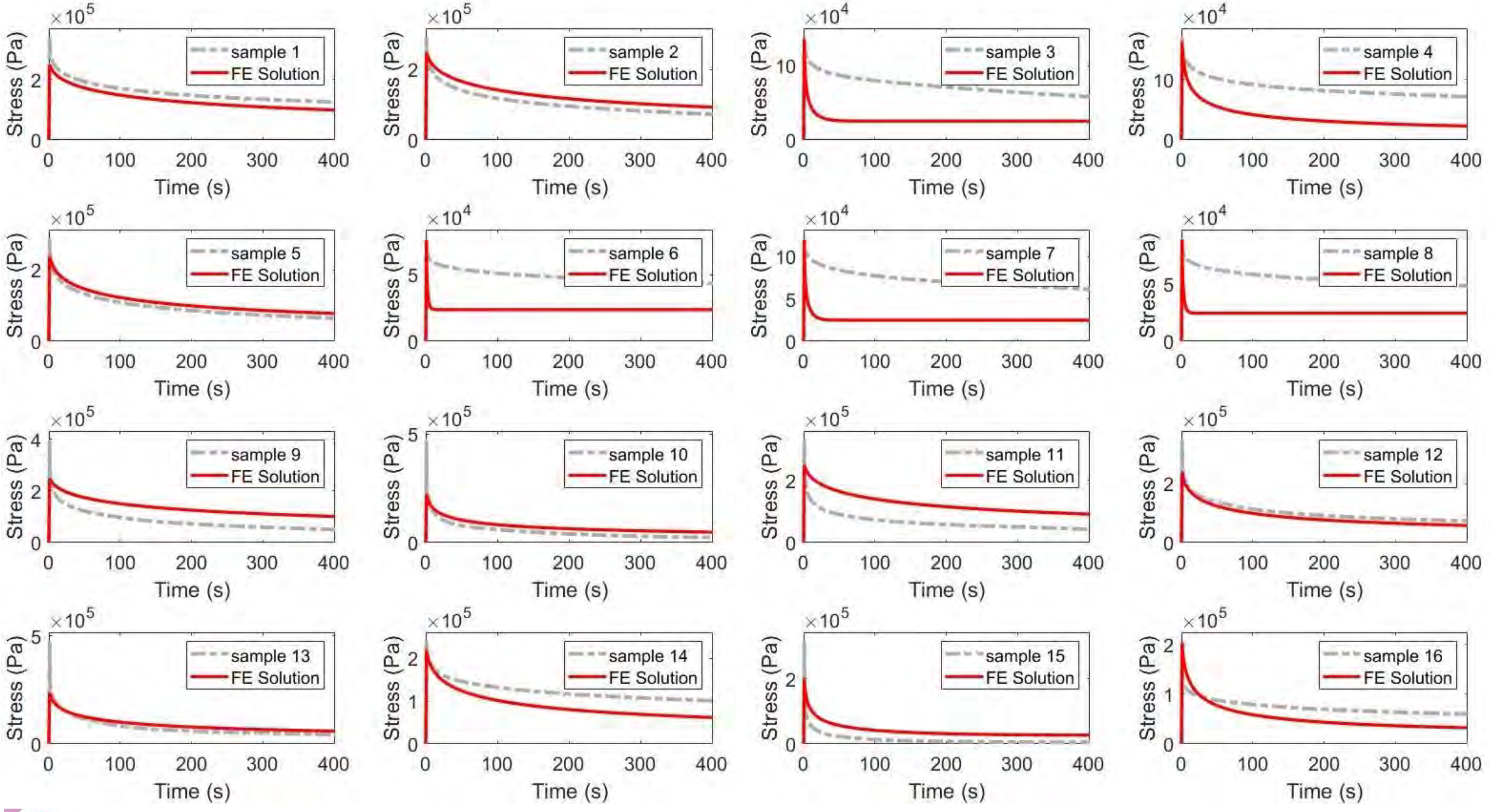

J: 0.12±0.13

Appendix C: Terzaghi verification (Sciume 2020)

p the pore pressure, p_0 the full load, z the height in the sample, h the height of the sample, t the time, c_v the consolidation coefficient, M the longitudinal modulus, S the inverse of the Biot modulus

1. Small strains and unidimensionnal
2. Saturated medium
3. Soil grains and fluid are incompressible
4. Homogeneous
5. Mechanical parameters are constant during the settlement
6. Unidimentionnal leakage, following Darcy's law
7. Linear link between effective stresses and volume variation of the soil
8. The soil has no structural viscosity or secondary settlement

$$\mathrm{p} = \frac{4p_0}{\pi}\sum_{k=1}^{+\infty}\frac{(-1)^{k-1}}{2k-1}\cos[(2k-1)\frac{\pi}{2}\frac{z}{h}]\exp[-(2k-1)^2\frac{\pi^2}{4}\frac{c_v t}{h^2}]$$

$$c_v = \frac{k^\varepsilon}{\nu^l(S+\frac{\beta^2}{M})}$$

$$M = \frac{3K^s(1-\nu)}{(1+\nu)}$$

$$S = \frac{\beta-\varepsilon_0^l}{K^s}+\frac{\varepsilon_0^l}{K^l}$$

Appendix C: Terzaghi verification (Sciume 2020)

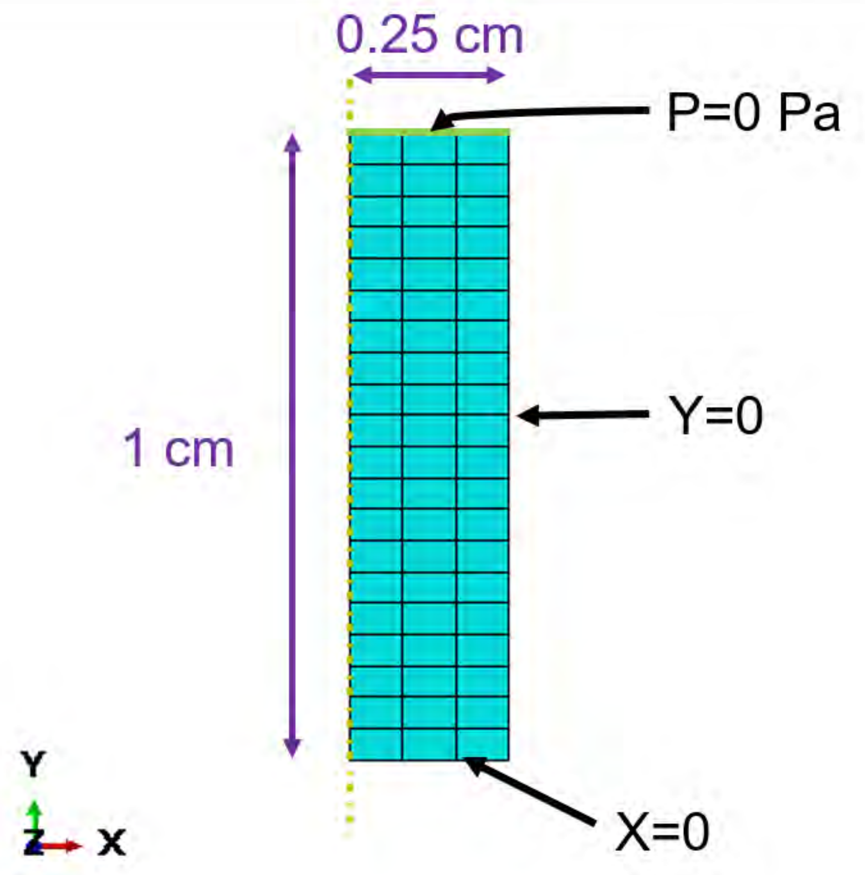

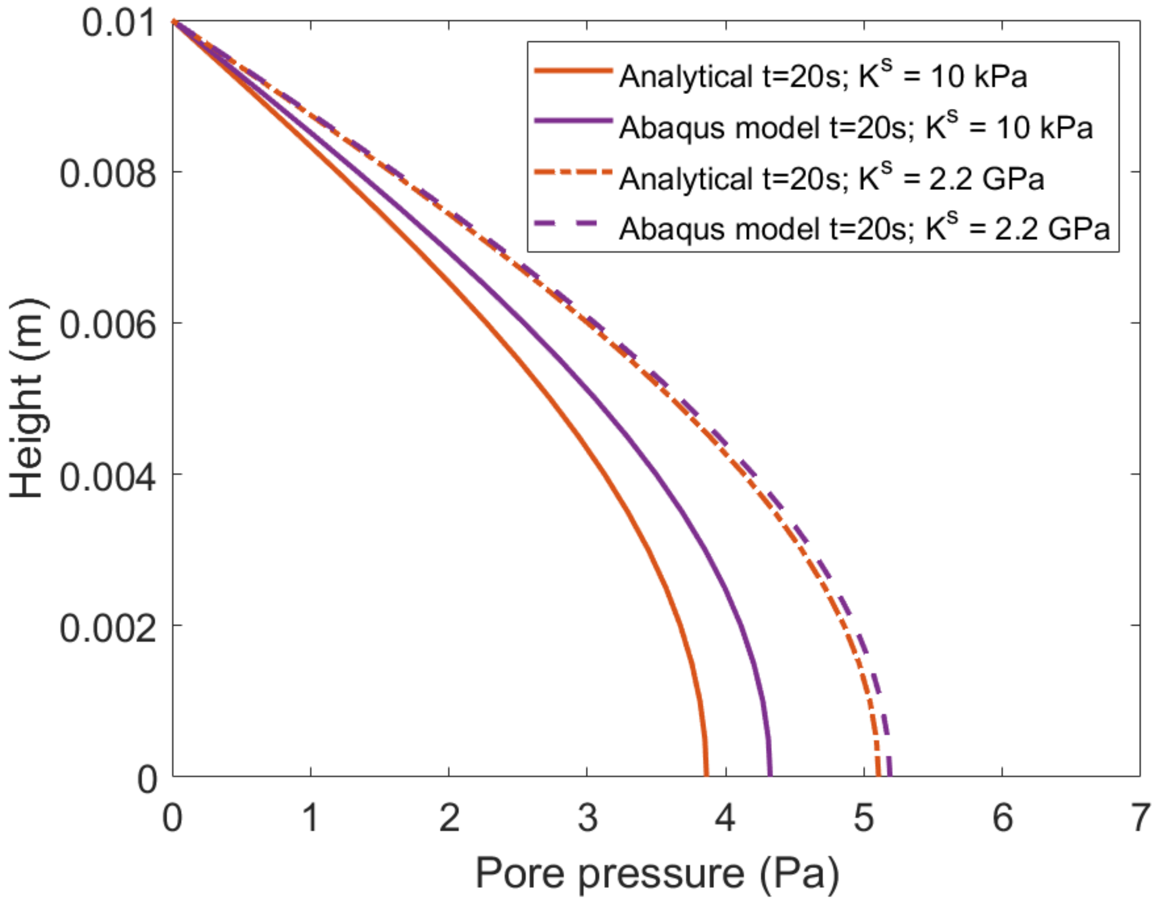

Appendix D: Evolution of the stress

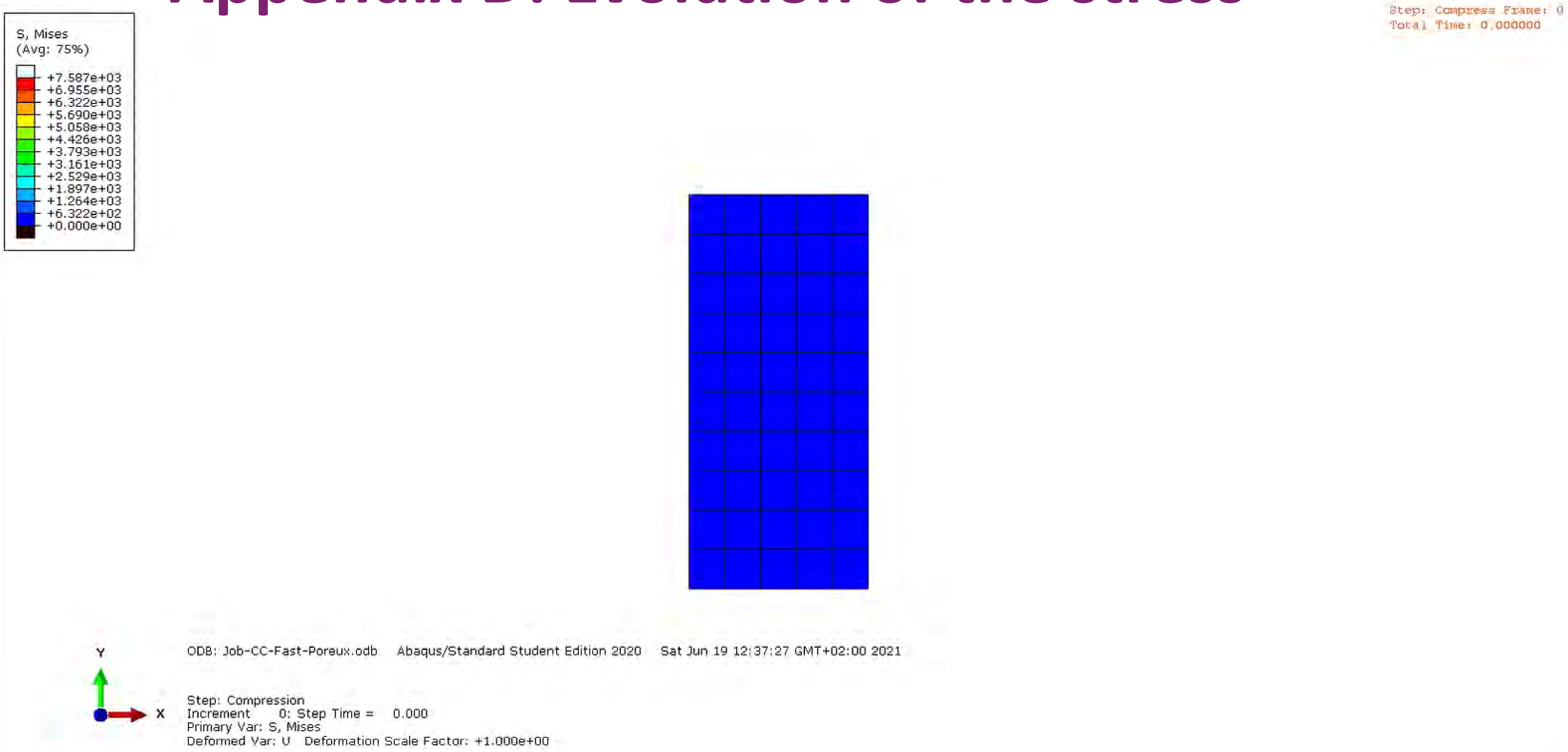

Appendix D: Evolution of the pore pressure

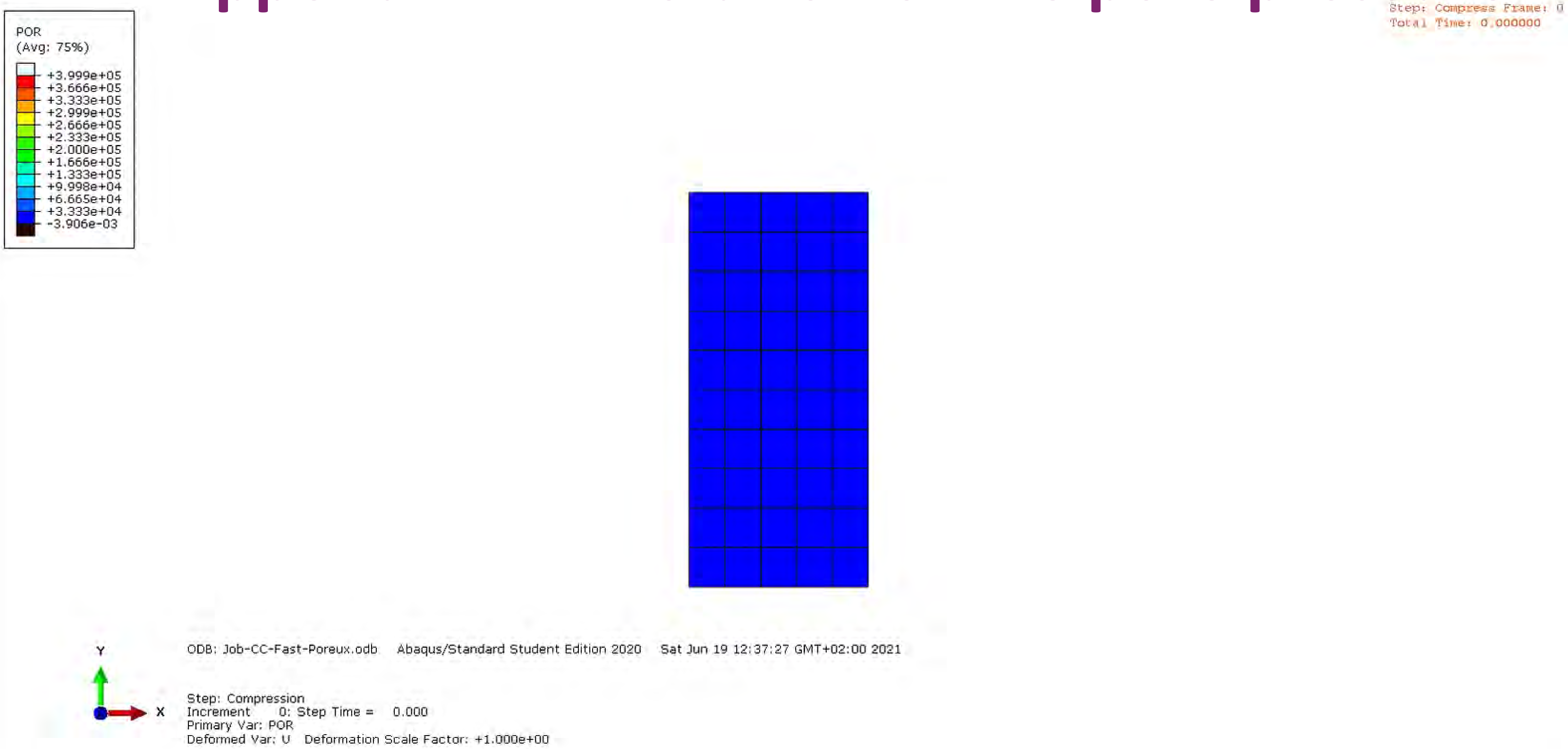

Appendix D: Evolution of the void ratio

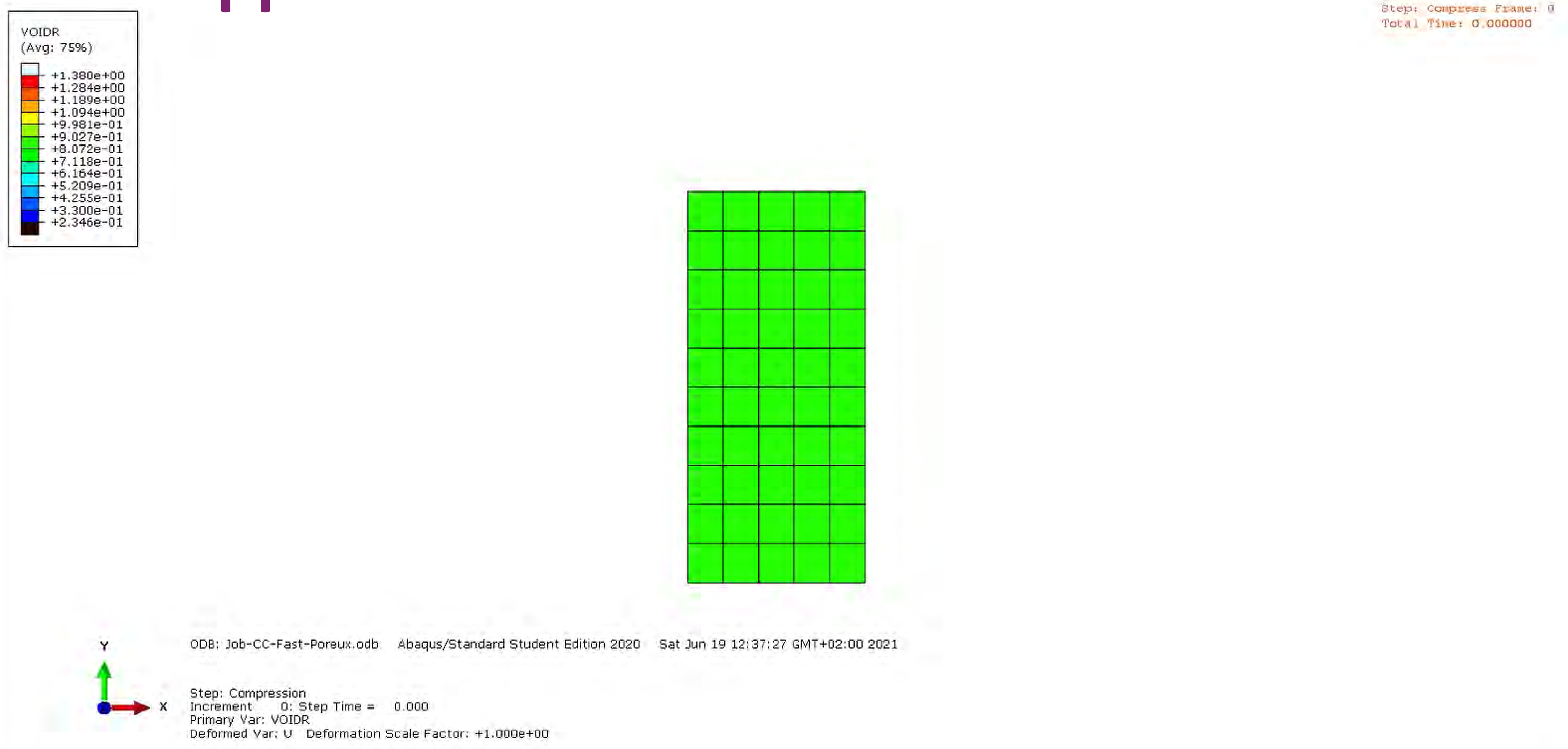

Appendix E: Material Laws Parameters

The possible role of poroelasticity in the apparent visco-elastic behavior of passive muscle tissue under compression: calibration of poroelastic material parameters to provide a mechanistic explanation of settlement

Final strain: 0.15
Fast strain rate: 0.15 s-1

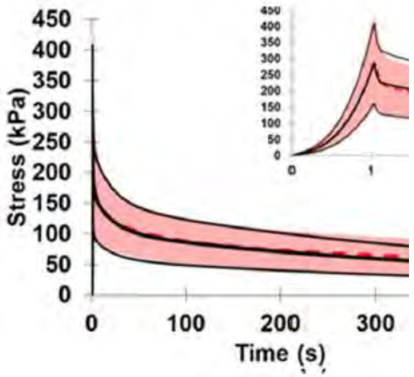

Final strain: 0.15
Slow strain rate: 0.015 s-1

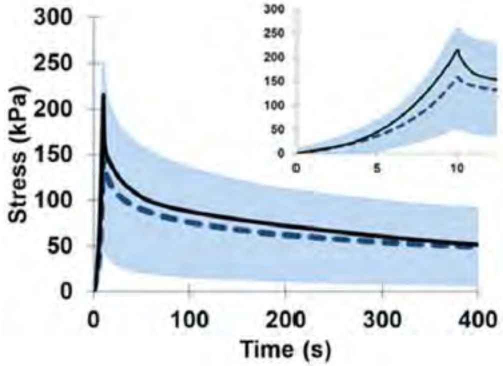

Law	Parameters Type	Parameter symbol	Value
Yeoh	Hyper-elastic (MPa)	C_{10}, C_{20}, C_{30}	$2.23e-5, 1.28e-4, 2.52e-5$
	Hyper-elastic (MPa^{-1})	D_1, D_2, D_3	105.9, 0.839, 0.0
Prony Series	Shear Coefficients (-)	G_1, G_2, G_3, G_4	0.741, 0.086, 0.093, 0.061
	Bulk Coefficients (-)	K_1, K_2, K_3, K_4	0.563, 0.150, 0.108, 0.147
	Time Coefficients (s)	$\tau_1, \tau_2, \tau_3, \tau_4$	0.05, 1, 20, 400

Final strain: 0.15
Fast strain rate: 0.15 s-1

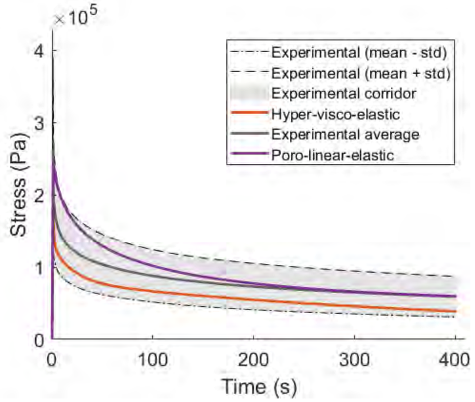

Final strain: 0.15
Slow strain rate: 0.015 s-1

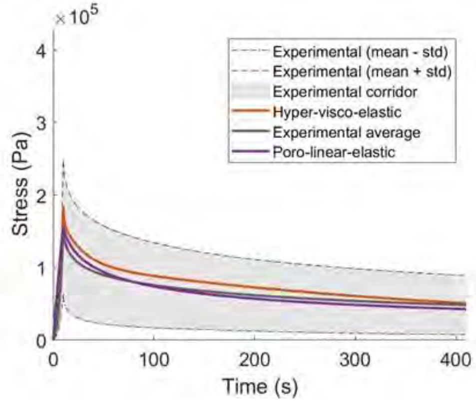

Solid Phase	Fluid Phase	
Young's Modulus (kPa)	Hydraulic permeability ($m^2Pa^{-1}s^{-1}$)	Void ratio (-)
12.89 ± 11.29	$(2.09 \pm 3.12) \times 10^{-13}$	0.469 ± 0.247
20.16 ± 8.54	$(1.94 \pm 5.71) \times 10^{-13}$	0.640 ± 0.325

Bibliography: Order of magnitudes

Authors	Type	Sample	Material Law	Phase		
				Solid Phase	Fluid Phase	
				E (kPa)	k ($m^2 Pa^{-1} s^{-1}$)	Void Ratio (-)
[Gras et al., 2012a]	Experimental	Human muscles	hyper-elastic	111 (min: 12 ; max: 292)	-	-
[Gras et al., 2012b]	Experimental (lateral compression)	Human muscles	Linear Elastic	1860 (min: 1020 ; max: 2790)	-	-
[Palevski et al., 2006]	Experimental (Indentation Test)	Porcine muscles	Transient shear modulus	2.4 (long term) 17 (short term)	-	-
[Wheatley et al., 2016]	Experimental (Permeability test)	Rabbit muscles	Poro-hyper-elastic	-	$(7 \pm 2) \times 1e-11$	-
[Gimnich et al., 2019]	Numerical	Muscle	Poro-elastic	-	$min: 4 \times 1e-14$ $max: 1 \times 1e-9$	-
[Argoubi and Shirazi-Adl, 1996]	Numerical	Human Cartilage and bone	Poro-elastic	$min: 1 \times 1e3$ $max: 10 \times 1e6$	$min: 1 \times 1e-20$ $max: 1 \times 1e-13$	$min: 0.1$ $max: 0.3$
Current study	Numerical	Porcine muscles	Poro-linear-elastic	16 ± 10	$(2 \pm 4) \times 1e-13$	(0.6 ± 0.3)

Conclusion and perspectives

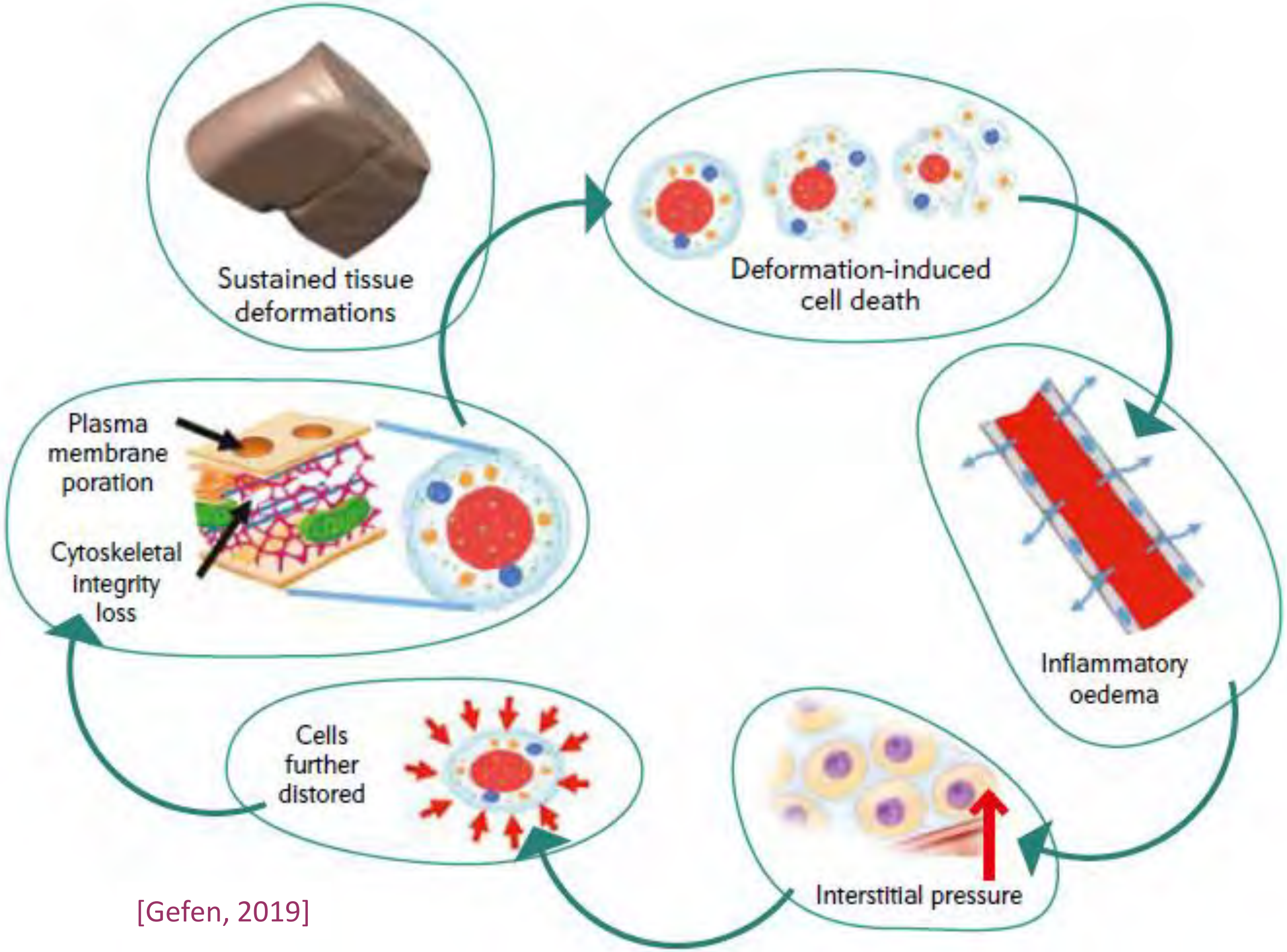

[Gefen, 2019]

Cell strain >> Inflammatory response of the tissue >>Plasme membrane poration >> cell death